

Review Article

An introduction to PVDF nanofibers properties, and ways to improve them, and reviewing output enhancing methods for PVDF nanofibers nanogenerators

Sedigheh Aghayari*¹

¹University, Sharif University of Technology, Tehran, Iran

Correspondence

*Sedigheh Aghayari, Tehran.

Email: 1415he@gmail.com

Funding Information

none

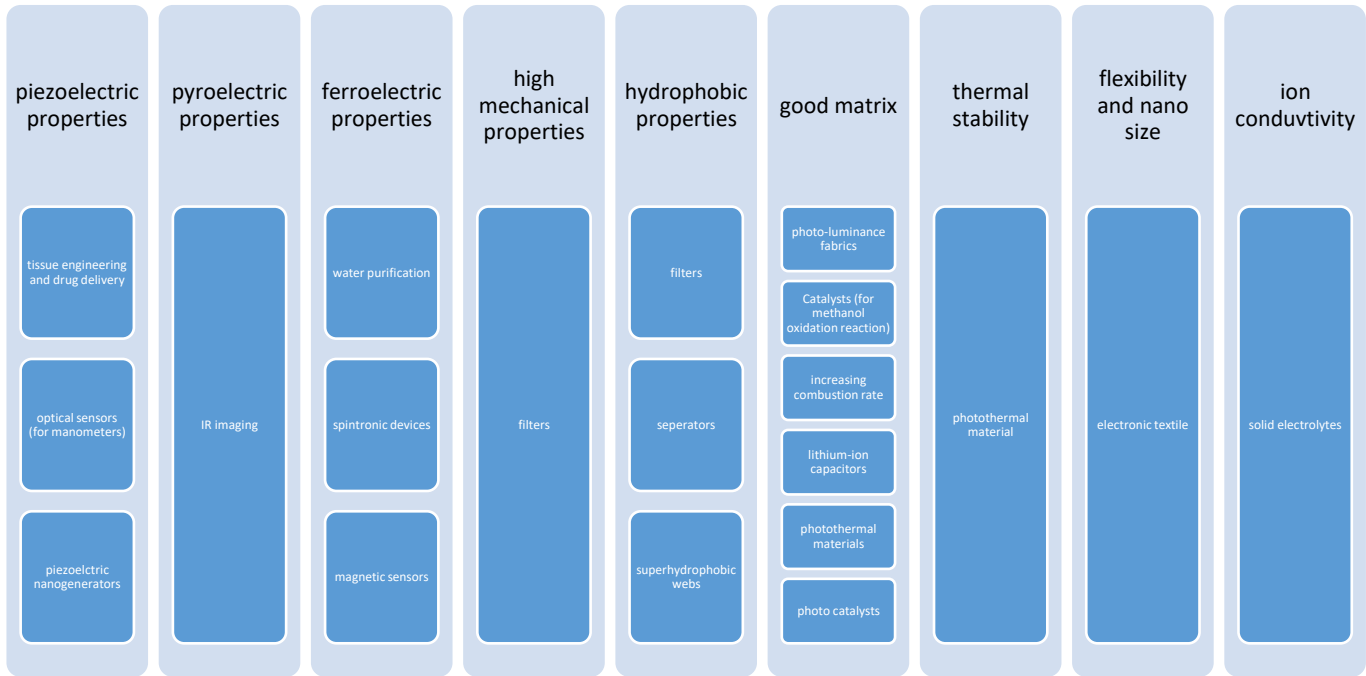
Abstract

PVDF has special piezo/pyro/ferroelectric, flexibility, low weight, biocompatibility, economical, good chemical/thermal, and high mechanical properties such as excellent nontoxic fiber/film formation. It has polar and nonpolar phases of α , β , γ , ϵ , and δ that the nonpolar α phase is the most stable one, but the β phase is the best of all because it has good piezo/pyro/ferroelectric properties. Copolymers are attractive because of their low weight, nontoxic, chemical acid resistance, flexibility, and ease of processing. These aspects result in their applications in many fields. They are used for piezoelectric nanogenerators, cooling/heating sensors, electronic devices (fuel cells, lithium-ion batteries (as separators), dye sensitive solar cells), filtration, oil/water separation, and photoelectric nanodevices. This review highlights the main aspects of the last decade's articles, and the focus is on the synthesis methods of PVDF nanofibers and their properties which results in their application in different fields of industry and especially focuses on finding ways to increase the output of PVDF nanofibers nanogenerators (weight/acoustic pressure nanogenerators).

KEYWORDS

PVDF, electrospinning, nanogenerators, piezoelectric.

Graphical table



Introduction

Due to the excellent properties of PVDF, nanostructures based on it have applications in smart wound dressing, smart machine seats, self-cleaning filters, cooling and heating sensors [1], electronic devices, ultrafiltration, heavy metals removal, photocatalysts, desalinate water osmosis, oil/water separation [2] and photoelectronic devices [3].

Electrospun nanowebs have a high specific surface area, adjustable porosity, interconnective pores, microscale interstitial distance, and flexibility because of their different sizes and morphologies. Due to these advantages, they are attractive in tissue engineering, sensors, wearable electronics, and water purification [4] but recently, other methods such as centrifugal spinning [5], blow spinning [6], and ... are attractive. Because of the limitations of electrospinning, including high voltage sources, in most cases, it requires toxic organic solvents and low production rates [5]. Depends on synthesis conditions, nanofibers can have different morphologies like mesoporous fibers [7]. These morphologies result in a higher specific surface of nanofibers that can enhance their properties special their sensing operation.

PVDF nanofibers with nanostructures give hydrophobic, controllable structural properties (length to diameter ratio, high surface to weight ratio, and small diameter (tens to hundreds nanometer)),

piezo/pyro/ferroelectric properties (easy to control by adjusting production parameters) that give more attention to them.

This review focuses on synthesis methods, properties, and applications of PVDF nanofibers.

PVDF nanofiber

The following is focused on PVDF nanofibers synthesizing methods, their main properties, and their application in other industries.

Many methods have been developed for the production of nanofibers such as centrifugal spinning [5], blow spinning [6], electrospinning [8], and so on. Most of the articles in the last decade focus on electrospinning with the polymer solution, but other methods have developed recently because of their limitations. Forcespinnig is a centrifugal spinning that uses centrifugal forces instead of high voltage to thinning a jet [5]. Two parallel concentric fluid flows, including polymer solution flow and compact airflow surrounding polymer solution, exist in blow spinning. Jet produces and thins with airflow and evaporates solvent fibers in the same direction of gas flow deposit. This method does not have high voltage despite electrospinning. [5]. Electrospinning with melt compares to the solution is more economical and environmentally friendly because of the absence of organic solvents and ease of process [8].

Investigating and utilizing PVDF nanofibers with different nanoparticles has been attractive recently. Better and multifunctional properties result from using other structures such as small molecules, polymers, and nanostructures.

The morphology of nanofibers can change with controlling production parameters, and it has a vital role in arising properties of the material. For example, nanofibers' morphology is very useful in piezo/pyro/ferroelectric properties because the reduction in diameter due to more thinning can increase the β phase [9]. Increasing specific surface area can benefit gas absorption [7]. To increasing the PVDF properties, different metal and metal oxide elements as dopants like Ce, MoS₂, etc. have been used.

Knowledge and utilizing of piezo/pyro/ferroelectric properties, hydrophobicity, and chemical and mechanical stability of nanostructures can develop sensors, nano/photoelectric devices, and other exciting applications.

Therefore, some details based on piezo/pyro/ferroelectric properties, hydrophobicity, and chemical and mechanical stability of recently developed PVDF nanofibers in various applications are discussed in the following.

Piezoelectric properties

Ceramic nanofibers with high piezoelectric properties do not have enough flexibility and wearing ability; therefore, using piezoelectric polymers is the solution. Among them, PVDF has the most piezoelectric properties but is not higher than ceramics. There are many methods for arising β phase, including mechanical drawing, thermal annealing, or electrical polling, but all of them have limitations for PVDF.

Methods to improve the piezoelectric properties of PVDF are a lot, such as electrospinning, and doping which are focused on in the following [10].

In electrospinning, dipoles are aligned along with layer thickness that results in the polarization of the layer.

For determining the piezoelectric properties of PVDF, investigating the β phase content is useful. For this work, FTIR, XRD, PFM, FESEM, and DSC can be helpful.

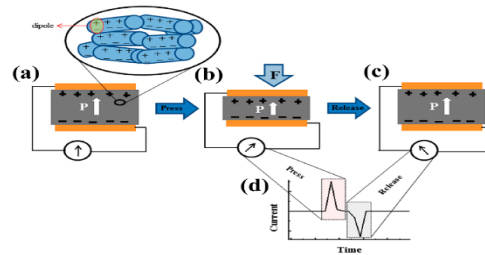


Figure 1 NG working mechanism [9]. Permission from [ACS Applied Energy Materials].

Utilizing pressure stresses results in the layer's polarization because of changing the overall momentum of dipole and thickness of the layer under pressure, and now charges produce and flow from the external circuit. After removing these external stresses, the polarization saves, and current in the opposite direction flows that make the inverse signal. Therefore, the output is the usual AC signal (figure 1) [9].

Figure 1 Working mechanism of the NG at (a) the initial state (enlarged view shows that the dipoles are aligned along the thickness direction), (b) pressed state, and (c) released state. (d) Press and release states are resulting in positive and negative peaks of AC generated from the NG [9].

FESEM is for investigating the morphology of nanofiber that the diameter of the nanofibers can extract from it. Results of the researcher's works are presented in figure 2 and table 1.

According to the results by doping, the conductivity of the solution increased, so the diameter of the nanofibers reduced, and the piezoelectric property increased but in sample 2, by increasing the solution viscosity, the diameter of the nanofiber increased. In sample 3 and the graphene, cerium ions were added too, which helped the diameter reduction.

For calculating the exact β phase content and investigating crystallinity, the FTIR test is good. To analysis the results, table 2 is helpful. There are many wavelengths for all phases but commonly bands at 840 are used for the beta phase and at 833 for the gamma phase which is very near to 840 and other bands are not very strong so, they can be not considered in the analysis [16]. Results of the researcher's works are presented in figure 3 and table 3. From the results, it is clear that after doping, the peaks for the beta phase got higher, but others got lower. So, FTIR can show encasement of the beta phase. There is a formula for calculating the content of each phase by calculating the baseline-corrected absorbance and wavenumbers for each phase but by looking at the curves we can see if the phases got stronger or not.

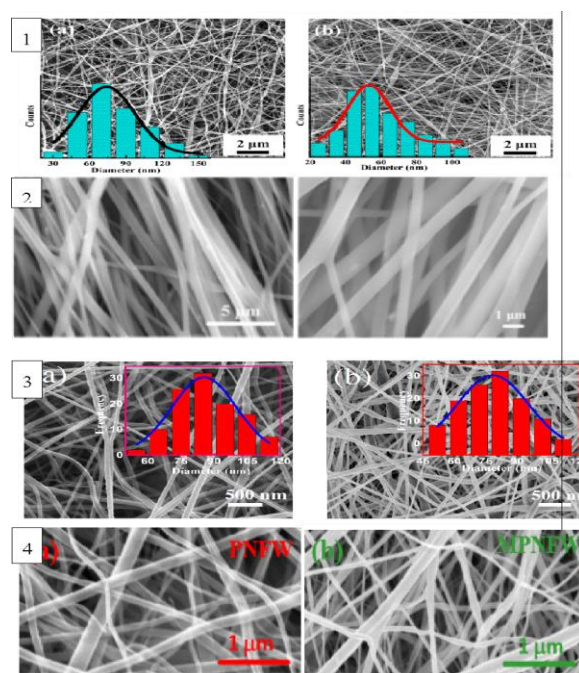


Figure 2 FESEM images of nanofibers with/without dopants respectively left and right sides: 1) TiO₂ [9], 2) BTO [10], 3) G [11] and 4) MoS₂ [12]. Permission from [ACS Applied Energy Materials, ACS applied materials & interfaces, ACS applied materials & interfaces and Energy Technology (5170270152628)].

Table 1 Diameters of nanofibers with/without dopants, column 4 is the diameter of PVDF nanofibers and column 2 is the diameters of PVDF nanofibers with dopants.

sample	diameter (nm)	sample	diameter (nm)	diameter changes (%)	source
PVDF/TiO ₂	-	PVDF	-	decreased	9
P(VDF-TrFE)/BTO	-	PVDF	400	-	10
PVDF/Ce ³⁺ /G	80	PVDF	85	-6	11
PVDF/MoS ₂	75±10	PVDF	107±5	-30	12
PPy/PVDF	325±143	PVDF	453±153	-28	13
PANI/PVDF	390±138	PVDF	453±153	-14	13

P-LGA/PVDF	2512±1182	PVDF	453±153	454	13
PVDF-ILS4	592±404	PVDF	321±152	84	1
PVDF/Ag	169±21	PVDF	156±13	8	14
PVDF/ZnO	195	PVDF	240	-19	15

Table 2 The wavelength of picks of different phases of PVDF [16]. Reproduced from [5155610858383], with permission from [Progress in Polymer Science].

Wavenumber (cm ⁻¹)		
α	β	γ
408	510	431
532	840	512
614	1279	776
766		812
795		833
855		840
976		1234

1	
---	--

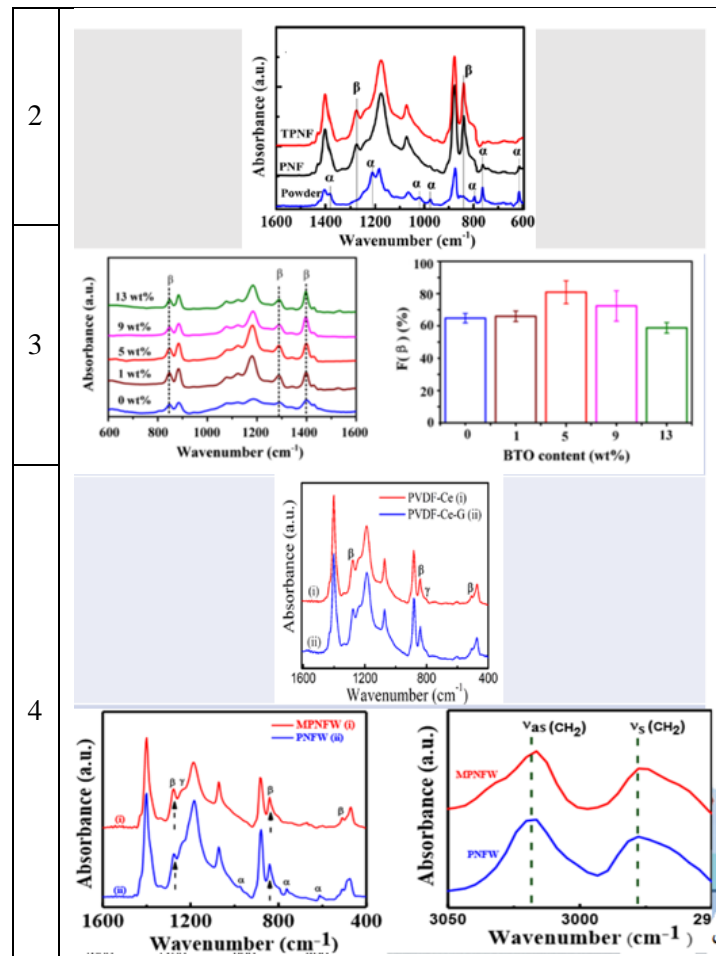


Figure 3 FTIR images of nanofibers with/without dopants respectively red and blue/black curves: 1) TiO₂ [9], 2) BTO [10], 3) G [11] and 4) MoS₂ [12]. Permission from [ACS Applied Energy Materials, ACS applied materials & interfaces, ACS applied materials & interfaces and Energy Technology (5170270152628)].

Table 3 Beta phase contents of nanofibers with/without dopants column 4 is the β phase content of PVDF nanofibers and column 2 is the β phase content of PVDF nanofibers with dopants.

sample	β phase (%)	sample	β phase (%)	β phase change (%)	source
PVDF/TiO ₂	-	PVDF	-	16	1
P(VDF-TrFE)/BTO	81	PVDF	65	16	11
PVDF/Ce ³⁺ /G	99	PVDF	96	3	12
PVDF/MoS ₂	95	PVDF	92	3	13
PPy/PVDF	83.5	PVDF	77.4	6.1	14
PANI/PVDF	83.6	PVDF	77.4	6.2	14
P-LGA/PVDF	85.3	PVDF	77.4	7.9	14
PVDF-ILS4	98.62	PVDF	76.04	22.58	2
PVDF/Ag	94	PVDF	83	11	15
PVDF/ZnO	92	PVDF	86	6	16

PVDF/Pt	99.9	PVDF	76	23.9	18
---------	------	------	----	------	----

According to the results by doping, the β phase increases that result in higher piezoelectric properties. Investigating the crystallinity is possible from this test. Analysis results of this test (for $K_{a1}=1.5405600\text{ \AA}$) according to table 4, is possible. In table 3 the peaks of different phases were mentioned, and each peak is belonging to a special crystal plane [16]. Results of the researcher's works are presented in table 5. When the peaks of each phase get stronger that means that this phase has been increased and this is a way to understand that if the process was successful to increase the special phase or not? In table 5, it is visible that adding any dopants resulted in higher beta phase content which means that all of the doping can result in higher beta phase content. So, XRD is a way to understand if the beta phase got higher or no?

Table 4 Degrees of picks of different phases of PVDF [16]. Reproduced from [5155610858383], with permission from [Progress in Polymer Science].

PVDF	2 θ (°)	Crystal plane
α	17.66	(100)
	18.30	(020)
	19.90	(110)
	26.56	(021)
β	20.26	(110) (200)
γ	18.5	(020)
	19.2	(002)
	20.04	(110)

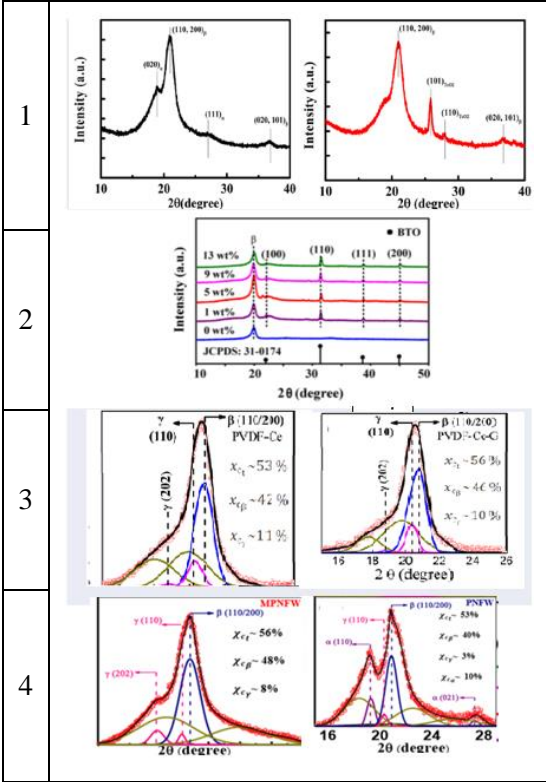


Figure 4 XRD images of nanofibers with/without dopants respectively left and right sides: 1) TiO₂ [9], 2) BTO [10], 3) G [11] and 4) MoS₂ [12]. Permission from [ACS Applied Energy Materials, ACS applied materials & interfaces, ACS applied materials & interfaces and Energy Technology (5170270152628)].

According to the results of the addition of additives, the piezoelectric property increased.

PFM is a simple method that uses contact mode for evaluating the single fiber piezoelectric constant. Effective piezoelectric constant $d_{33, \text{eff}}$ achieves from the following equation where A, V, and ϵ are respectively amplitude, AC voltage, and correction factor that illustrates by alternative electrical polling of standard lithium niobate. High $d_{33, \text{eff}}$ illustrates high piezoelectric properties [10].

The researcher's work results are presented in Table 5. When the effective piezoelectric constant gets higher it means that the piezoelectric properties got stronger. In table 5, all dopings resulted in a higher effective piezoelectric constant, and PFM could approve that. For this section, an electrospun layer with the electrode(s) is used, and by applying pressure such as human hand force, the pressure converts into electricity, and now the electrical voltage can be measured.

Table 5 Comparing outputs of different researches for nanofibers with/without dopants.

Sample	Force (N)	Area (m ²)	Pressure (Pa)	Output voltage (V)	Sensitivity (V/KPa)	Current (nA)	Source
PVDF/no TiO ₂	5	0.006	833.33	7	8.4	104	[9]
PVDF/no BTO	-	-	7000	-	-	4.8	[10]
PVDF/no G	8	825	6600	4.5	0.68	-	[11]
PVDF/no MoS ₂	7	1257.142	8800	2.5	0.28	-	[12]
PVDF/TiO ₂	5	0.006	833.33	11.5	13.8	176	[9]
PVDF/BTO	-	-	7000	-	-	12.5	[10]
PVDF/G	8	825	6600	11	1.66	-	[11]
PVDF/MoS ₂	7	1257.142	8800	14	1.59	-	[12]

As seen in table 5 by doping, piezoelectric output increased, and the effect is entirely adaptive with the results of previous tests.

It concluded that FESEM/SEM, FTIR, XRD, PFM analysis or measuring the voltage, and current outputs of piezoelectric tests help to find that the piezoelectric property has enhanced or not. It conducted that doping is a suitable way of improving the piezoelectric effect and oil separation efficiency of electrospun PVDF webs from the results. There are other methods for improving piezoelectric output too, such as increasing specific surface area (by mesoporous nanofibers [18], penetrated electrodes [10], and plasma treatment [19]), benefiting the test and layer conditions [20] (layer thickness, kind of polymer, the diameter of nanofiber, nanofiber alignment in web, area of the

layer, and finding the conditions which make higher output), and the electrode (kind of electrode [21] and kind of method of applying the electrode on the layer [22]) which is a subject of the next article.

Ferroelectric property

In contrast with different nanoparticles such as TiO_2 , SrTiO_3 , BaTiO_3 , and, ferrite nanoparticles have superior efficiency to increase the electroactive phase of the PVDF and its copolymers. These nanoparticles can increase the magnetic, ferroelectric, and dielectric properties of PVDF. NiFe_2O_4 is one of the essential ferrite materials that have application in MRI contrast agents, media with the capability of saving high magnetic density, ferrofluid, color imaging, catalysts, and microwave devices. High information saving efficiency, nanomagnetic, and ferroelectric results in good energy production from the piezoelectric property when they incorporate in PVDF [23].

Adding nanoparticles, especially ferrite nickel, results in the nucleating of the ferroelectric phase combined with phase conversion due to the corporation of nanoparticles and increases the crystallinity. However, trapped particles in the amorph phase of the polymer result in spherulite growth [23].

Ferroelectric properties of all the samples tested by a system (figure 5). Particular vibrations (15-45Hz) were applied to the samples with the aid of the frequency generator. Amplifier for amplifying the vibrations and transfer them attached to vibration shaker. Sample with conductive wires on both sides on the top of the shaker kept with the weight of 2.5N. According to vibration frequency, the shaker did the shakes, and weight contributes to the sample's pressure force. These forces show the electrical voltage by changing the dipole moment, and the data receiving system records these results. With a resistant box attached to the sample, the produced voltage can maximize before recording [23].

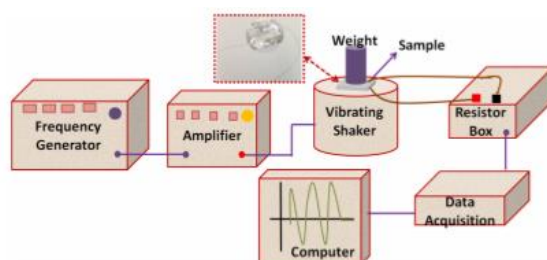


Figure 5 Schematic representation of the piezoelectric experimental setup [23]. Reproduced from [5155600761114], with permission from [Materials Chemistry and Physics].

The maximum dielectric constant of nanocomposites with 1wt% NiFe_2O_4 was 118 in 1Hz, which was 24 times higher than nanofibers. By adding 2wt%, additive output voltage was 4V [23].

Magnetoelectric devices have magnetic sensors, multistate memories, electric field controlled ferromagnetic resonance devices, and actuators. It is because of the dielectric polarization property by applying a magnetic field and/or induce magnetization with an external field [23].

For determining the magnetoelectric properties of PVDF/PMMA- Fe_3O_4 nanofibers, PFM (by applying the magnetic field determines the piezo, and magnetoelectric properties) was used. With the addition of nanoparticles, the diameter increased. Amplitude compared to iron oxide nanoparticles was much narrower. It is a sign of the effect of magnetic

field on piezoelectric response and magnetoelectric effect (to deliver the appropriate electrical signal for nerve and tissue cells in biomedical) [24].

$\text{Co}_{0.5}\text{Ni}_{0.5}\text{Fe}_2\text{O}_4/\text{PVDF}$ nanofibers due to the doping have a higher β phase compared to

PVDF nanofibers influenced the ferroelectric properties of the layer. VSM (Vibrating Sample Magnetometer) method used for determining ferroelectric properties (figure 6). The stability of the magnetization of nanoparticles increased due to the polymer's nonmagnetic nature, so the resulting web is useful for water purification, spintronic devices, and magnetic sensors [25].

Ferroelectric properties are also present in the tetragonal barium titanate [26] and gold [27] nanoparticles.

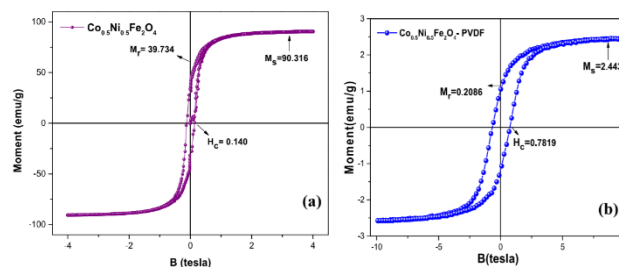


Figure 6 VSM plots of (a) $\text{Co}_{0.5}\text{Ni}_{0.5}\text{Fe}_2\text{O}_4$ pristine nanoparticles and (b) $\text{Co}_{0.5}\text{Ni}_{0.5}\text{Fe}_2\text{O}_4$ -PVDF nanofiber membrane [25]. Reproduced from [5155601504764], with permission from [Nano-Structures & Nano-Objects].

Dopamine-functionalized BaTiO_3 / BaTiZrO_3 / BaZrO_3 -PVDF nanofibers had higher β phase content and better dielectric, ferroelectric (figure 7), and mechanical properties due to doping. They are appropriate for storing media in electrical devices such as memories with random access ability [28].

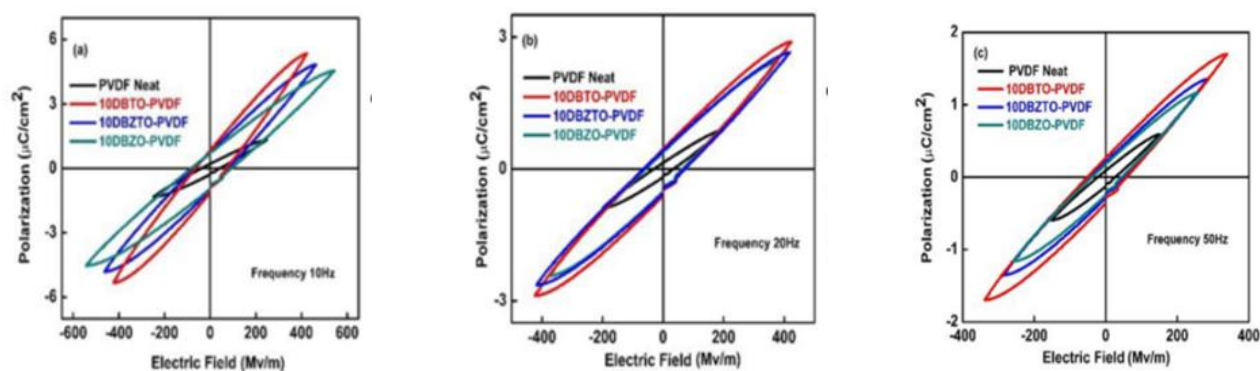


Figure 7 P-E loop of DBTO/DBZTO/DBZO-PVDF nanofibers at a different frequency (Time) (a) 10 Hz, (b) 20 Hz, and (c) 50 Hz [28]. Reproduced from [5155590564619], with permission from [Journal of Alloys and Compounds].

Pyroelectric property

Due to its properties, PVDF has applications in tactile sensors, energy harvesters, and IR imaging. PVDF has poor absorption in the visible region and near to IR, which avoids effective conversion of light to heat and then to an electrical signal. To overcome this problem, gold nanocages in nanofibers were used, so strong absorption resulted. Combine this method with electrospinning resulted in higher β phase content and better piezo/pyroelectric properties. Nano cages could give the nanofibers ability to convert light into heat and then into electricity, so it is good for sensing light. By applying tactile force and IR radiation, the output voltage 12.6 times increased (7.2V), so a piezo/pyroelectric hybrid sensor was conducted [29].

Plasmonic nanomaterials for applications from photonic to medical have developed due to localized surface plasmon resonance (LSPR) and properties related to them. An example of them is nanostructures based on gold with a wide range of shapes of non-spherical or complicated structures for the production of adjustable LSPR peaks in visible and near IR regions. Among them, gold nanocages with hollow space and porous walls are very attractive because their LSR usually makes them absorb rather than scatter. The absorption peak is adjustable precisely in the 400-1200nm region by controlling the wall thickness than all dimensions. These nanocages with strong absorption are efficient photothermal converters for converting a photon to phonon or heat [29].

Strong electrostatic interaction between nanoparticles with a positive charge and negative charge of the F atoms in the polymer chain can make interfacial polarization in the crystalline phase named β [29].

Gold nanoparticles are useful for changing the piezo/pyro/ferroelectric properties of PVDF [23].

Wettability properties

In lithium-ion batteries (as separators), in addition to high porosity, the good intrinsic desire between separator and electrolyte is necessary for electrochemical operation because good wetting ability can help faster lithium-ion transfer. The wetting ability of the webs with scattering 10 μ L of the liquid electrolyte was evaluated (figure 8). Wetting of the commercial sample was limited, but others wetted thoroughly in 2s. The contact angle of the samples of PE, PVDF, $\text{Al}_2\text{O}_3/\text{SiO}_2/\text{PVDF}$, $\text{Al}_2\text{O}_3/\text{PVDF}$, and SiO_2/PVDF were 25.1°, 18.3, 18.3, 16, and 46.3 respectively (figure 9) [8].

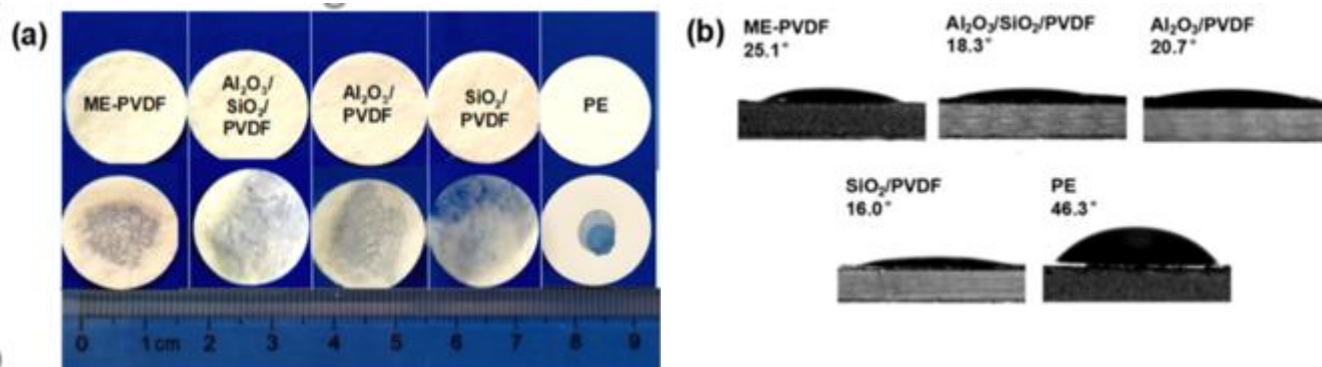


Figure 8 (a) Photographs of the wetting behavior. (b) Initial contact angles of the ME-PVDF, $\text{Al}_2\text{O}_3/\text{SiO}_2/\text{PVDF}$, $\text{Al}_2\text{O}_3/\text{PVDF}$, SiO_2/PVDF , and PE membranes with the liquid electrolyte [8]. Reproduced from case number [CSCSI0026247] with permission from [ACS Omega].

This can be due to the polar bands (C-F) in PVDF that prepare strong interaction with polar electrolytes. In contrast, PE web prepared from hydrophobic polyolefin resulted in low wetting with polar liquid electrolyte. [8].

PVDF-HFP nanofibers have hydrophobic webs due to the intrinsic hydrophobic nature and surface nano-roughness of nanofibers morphology. Utilizing Zwitterionic/PVDF-HFP and Zwitterionic/PVDF-HFP/Ag webs resulted in hydrophobicity reduction. The static water contact angle test was done with drops of nonionic water (5 μL) [4].

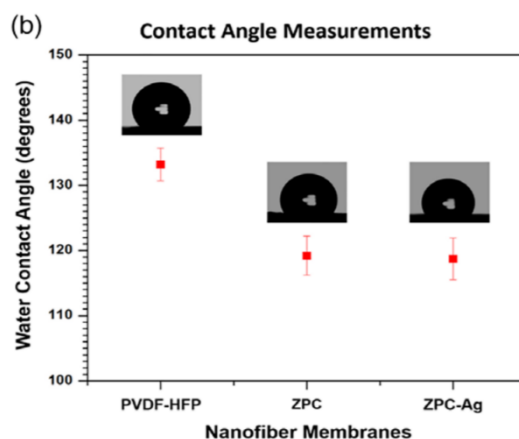


Figure 9 Static contact angle made by water droplet (5 μL) on PVDF-HFP, ZPC, and ZPC-Ag membranes [4]. Utilizing CNT [6, 30] or plasma treatment [19] is a way to have (super)hydrophobic webs. Reproduced from [5155610160794], with permission from [Journal of Applied Polymer Science].

In the $\text{Fe}_3\text{O}_4/\text{PVDF}$ nanofiber web, the hydrophobicity of the web changed by changing the nanoparticle concentration or electrospinning voltage.

For $\text{rGO}/\text{TiO}_2/\text{PVDF}$ webs, the water contact angle test was done (figure 10). The water contact angle for the web with rame-hart DROPimage was done at room temperature by dropping a 2 μL of nonionic water on the webs. Average of five measurements recorded. Welch's two-sample t-test was also done. Results showed that the contact angle was reduced by increasing the concentration of nanoparticles. This was because of nanofibers' surface morphology, and diameter that had an essential rule in the web's hydrophobicity. The average roughness of webs increased by increasing the nanoparticle concentration. By these nano-roughs, the surface tension and water contact angle were reduced [31].

Also, modifying these nanofibers with 1H, 1H, 2H, 2H-perfluorodecalin trimethoxysilane could make more hydrophobic even superhydrophobic webs (in -2kV or 10kV the contact angle was 153° [32].

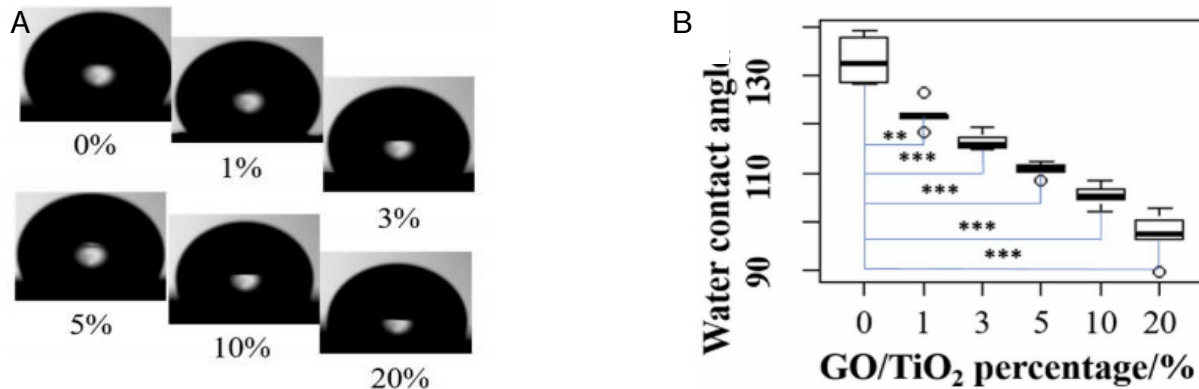


Figure 10 A) 0-20% samples, are water contact angle of the samples (PVDF/GO/TiO₂ nanofiber webs with a rGO/TiO₂ of 0%, 1%, 3%, 5%, 10%, and 20%). B) The water contact angle of samples and Welch two-sample t-test results ($n = 5$) [31]. Reproduced from [5155591390124], with permission from [Polymer].

Mechanical properties

PVDF webs have excellent mechanical properties, but for improving them, doping is helpful. GO, and TiO₂ are brittle materials, but PVDF is a ductile one so, by doping a mixture of both properties (more flexibility because of PVDF and more strength because of GO and TiO₂) obtain but the percentages of each material should be optimized otherwise the composite got near to brittle or ductile which is weird. Stress-strain curves of rGO/TiO₂/PVDF webs (figure 11) showed linear elastic behavior at first (lower than 3wt% nanoparticles) and then showed nonlinear behavior till failed. It is similar to nonwoven fabrics. The linear elastic step got smaller by increasing the nanoparticles' concentration, and the nonlinear one got bigger [31].

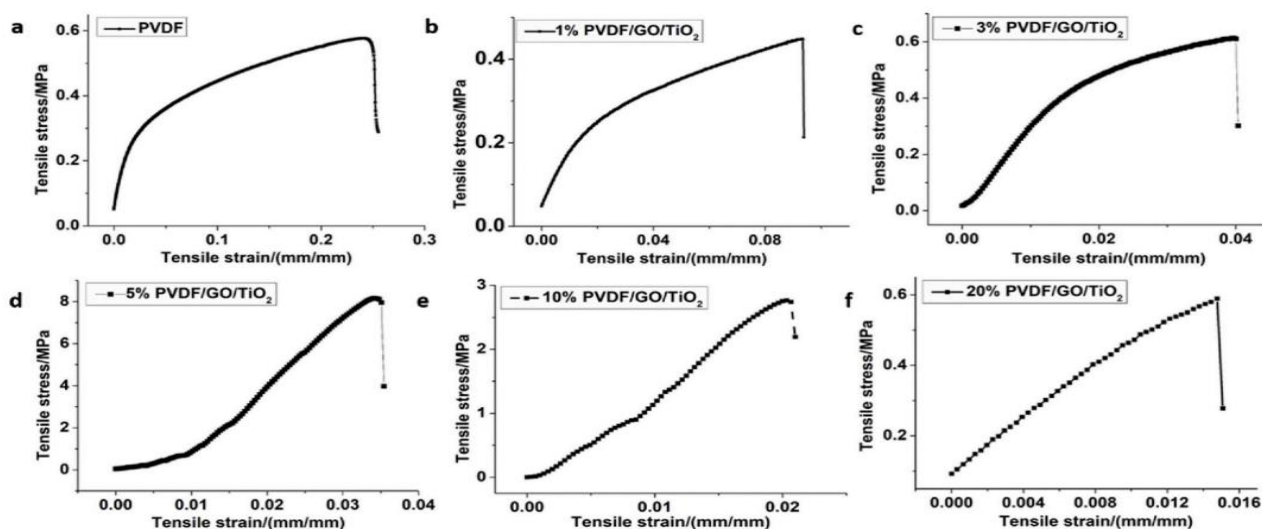


Figure 11 a-f) Tensile strain-stress curve of samples (PVDF/rGO/TiO₂ nanofibers webs) of varying rGO/TiO₂ concentrations [$\text{rGO/TiO}_2 \text{ \%} = (\text{rGO/TiO}_2 \text{ amount/g}) / (\text{PVDF amount/g}) \times 100\%$] of 0%, 1%, 3%, 5%, 10%, and 20% [31]. Reproduced from [5155591390124], with permission from [Polymer].

Stress-strain, force till failure, tension till failure, and yang modulus curves of TiO₂/PVDF webs are presented in figure 12. The stress-strain curve showed linear elastic behavior under low strain and then showed nonlinear (usually

increasing trend) behavior until it failed. It is similar to nonwoven fabrics. Force and tension till failure by increasing the nanoparticles concentration increased (due to filling the surface defects of the nanofiber by nanoparticles but after 3wt% reduced because of the adhesion of nanoparticles on the nanofiber surface that made it rigid) despite the yang modulus, so the best mechanical properties were for the 3wt% nanoparticles [2].

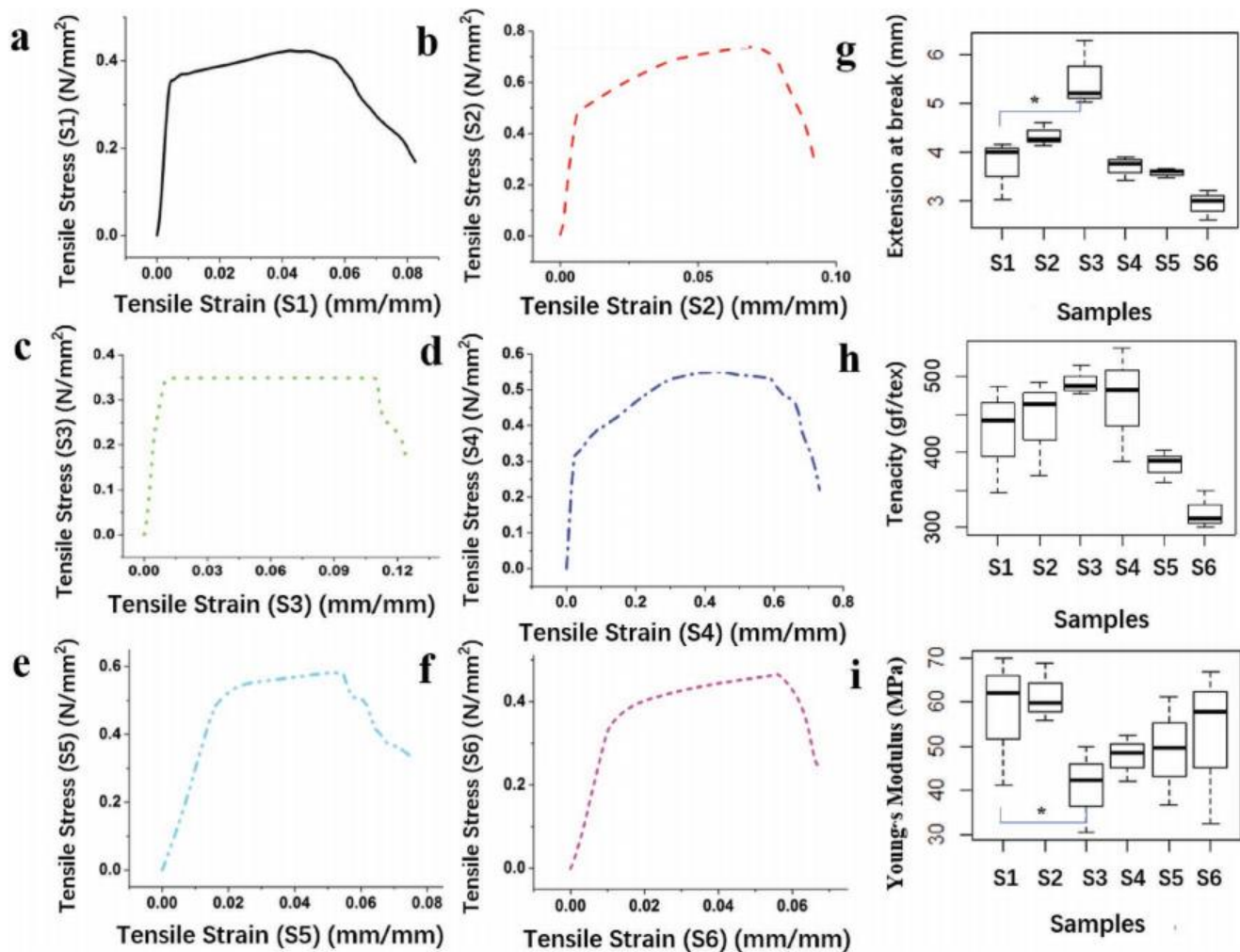


Figure 12 a–f) Sample a–f, shows tensile strain–stress curve of samples (PVDF/TiO₂ nanofibers webs) with varying TiO₂ concentrations of 0%, 1%, 3%, 5%, 10%, and 20%, respectively. g) Average extension at the break for samples and Welch two-sample t-test results (n = 3). h) Average load at the break for samples and Welch two-sample t-test results (n = 3). i) Average Young's modulus of samples and Welch two-sample t-test results (n = 3). Note: “*” means $p < 0.05$, which indicates significant difference exists at a 95% confidence level [2]. Reproduced from [5155620623948], with permission from [Particle & Particle Systems Characterization].

The focus is on the applications of the PVDF nanofibers such as sensors, photocatalysts, and lithium-ion batteries, which PVDF due to its excellent properties inter to these field.

PVDF based sensors

PVDF, because of its piezo/pyro/ferroelectric properties, has application in many sensors. In the following investigating of some researches in the subject.

Ce³⁺/PVDF nanofibers use in pressure sensors. High pressure resulted in modification of spectral splitting, intensity, width in half of the maximum of the emission peak, and luminance lifetime. It is enough for applications like manometers that need pressure calibration [5]. There are some examples of pressure sensors in table 6.

Table 6 Various Lanthanide doped optical pressure sensors [5]. Reproduced from [5155610294699], with permission from [Sensors and Actuators A: Physical].

Material	Method Merits	Demerits	Optical pressure Sensitivity	
Ce ³⁺ doped Fluorapatite Eu ³⁺ doped LaAlO ₃	λ_{em} -Centroid shift and peak broadening Shift in charge transfer transition	Very high-pressure sensitivity High linearity, Simple approach of using variation in charge transfer state Simple	Limited to 30GPa Low pressure sensitivity, Complexity due to Multiple peaks	0.67 nm/GPa 14.4 cm ⁻¹ /kbar
Eu ³⁺ doped Y ₂ O ₂ S	Shift in charge transfer transition		pressure in investigations extends only up to 24 GPa	–
BaWO ₄ :Ce single crystal	Host emission intensity	Singular emission peak	Not much change in spectral profile in terms of peak position and width, lower sensitivity	–
KMgF ₃ :Eu ²⁺	Change in Eu ²⁺ spectral profile	Singular emission, Suitable for multi cycle pressure experiments,	Low pressure range upto 30 GPa, issue with toxic character of fluorine, issue in low temperature	–0.815 cm ⁻¹ / kbar
Nd ³⁺ :Gd ₃ Sc ₂ Ga ₃ O ₁₂ crystal	Change in Nd ³⁺ spectral profile	NIR P-T sensor in anvil cells at low temperatures and from ambient pressure up to 12 GPa	Several peaks, limited to low pressure zone	–8.8 cm ⁻¹ /GPa
LaPO ₄ /YPO:Yb ³⁺ –Tm ³⁺	Change in the up-conversion emission profile of Tm ³⁺ Change in Sm ²⁺ spectral profile	High pressure sensitivity	Multiple peaks, complex phenomenon	–
SrB ₂ O ₄ :Sm ²⁺ nanoparticles		Sm ²⁺ -based contactless pressure nano-sensor allows a very accurate pressure sensing (± 0.01 GPa)	Data available for P up to 25 GPa only, lack of singular emission	0.24 nm/GPa
Cerium nitrate doped PVDF fiber	Change in Ce ³⁺ spectral profile	Singular emission, can work as low as well as high pressure sensor, wide linear dynamic range	Moderate pressure sensitivity	0.28 nm/GPa
Ammonium Cerium sulphate doped PVDF fiber	Change in Ce ³⁺ spectral profile	Singular emission, can work as low as well as high pressure sensor	low pressure sensitivity	0.10 nm/GPa

PVDF/AuNC hybrid device for recognizing the force and light was used simultaneously. This doping resulted in higher β phase content and piezoelectric response. The presence of nanocage in nanofibers gave them the ability to change the light to heat and then into electricity, so a piezo/pyroelectric hybrid sensor resulted [29].

Operation of the PVDF-HFP/(10-20wt%) BTO electrospun nanofibers under the alternative pressure of 20kPa considering electrical poling and nanoparticle concentration investigated. In the 10-20wt% region, piezoelectric properties got better, but after that, the nanoparticles' clustering was reduced. In 20wt%, the output voltage, current, and power were 9.63V, 0.52 μ A, and 7892.2nW, respectively. After electrical poling, the output voltage, current, and power results were 11.7V, 20.56 μ A, and 1115.2nW, respectively, which after rectifying was enough to lighten on a small LED bulb [26].

Electrospun PVDF-HFP/NiFe₂O₄ (with 1,2 and 3wt%) nanofibers resulted in better alignment of dipoles and phase conversion. In 1wt%, the web had a maximum dielectric constant of 118 in 1Hz that was 24 times higher than PVDF-HFP nanofibers. In 2wt%, the output voltage was 4V, so that it can apply in piezoelectric devices [23].

PVDF/nano clay (15wt%) nanofibers had 90% electroactive phase and had output voltage and power density of 7V and 68 μ A/cm², respectively [33].

Composite nanofibers of PVDF/2wt% Ce-Fe₂O₃ and PVDF/2wt% Ce-Co₃O₄ were prepared. Incorporating magnetic nanoparticles had a substantial effect on nanofibers' structural properties, especially β and γ phases of the polymer and adjusting of interfacial due to the increase of electrostatic interaction of filler-polymer. The outputs were 20V (0.01 μ A/cm²) and 15V, respectively, under 2.5N force. Nanoparticle size, filler-polymer interaction, and ion-dipole were influenced the produced piezoelectric power [34].

PVDF/BiCl₃ (2wt%) had output voltage, current, and surface power density of 1.1V (4.76 higher than PVDF), 2 μ A, and 0.2 μ W/cm² and could charge a capacitor by a bridge rectifier, and lightening on a red LED [35].

Electrospun PVDF nanofibers followed by hydrothermal producing ZnO (in the form of nanorods on the fiber) were achieved. The nanogenerator of the resulted web could convert sound (140 Hz, 116 dB) into electricity (1,12V, 1.6 μ A and 0.2 μ W cm⁻²) [36].

PVDF/AgNP (15wt%) nanofibers could increase the electroactive phase and gave the power of 7×10^{-4} W to convert sound to electricity [14].

PVDF/ZnO nanofibers had an output voltage of 4.8V under a wind force of 145Pa [15].

A solution of DMF and THF with different ratios was used to prepare PVDF/NP-ZnO nanofibers, and a lower concentration of ZnO and polymer and the same ratio of solvents gave the best fibers. By evaluating the effect of the process parameters, found that in smaller distances, the flow rate should reduce to result in more uniform fibers without beads or spraying. The maximum output power of the best sample was 32nW/cm². More uniform and stretched fibers gave higher outputs of voltage and current [37].

Other applications based on the PVDF nanofibers

PVDF nanofibers can be used in tissue engineering and drug delivery. As an example, PVDF nanofibers can be used in bone repair because of their flexibility and electrical microenvironment. It can be better when they dope with other piezo materials for example BTO [38].

Photo-luminance of rare-earth ion Eu^{3+} incorporated as well in polymers such as PVDF and PEO can be used to produce electrospun nanofibers [3].

PVDF/ Eu^{3+} nanofibers have a good emission spectrum because of 5D_0 to 7F_2 transfer which is responsible in front of luminance of Erium with a high-intensity ratio (2.61) (the ratio of above transfer to 5D_0 to 7F_1) which was higher than PEO/ Eu^{3+} nanofibers. It is due to the perfect dispersion of Erbium ions in PVDF chains that increasing interaction between them. The population of ions in PVDF was more than PEO. The application of these nanofibers is in photo-luminance fabrics and textiles. The presence of PMMA and PVDF in $\text{Eu}(\text{TTA})_3\text{phen}$ complex increased the sensitive fluorescent transfer intensity of 5D_0 to 7F_2 in the complex due to the effect of polymer on coordination ions that is the possibility of energy transfer of electrical dipoles that resulted in increasing of luminance with 612nm peak [39].

Metal catalysts materials with nanostructures and high specific surface area are appropriate for methanol oxidation reaction as catalysts with application in direct methanol fuel cells. Graphene is a 2D carbonic matter and is the best matter for platin cells due to its excellent electrical conductivity, high specific surface, and unique properties. Agglomeration of graphene can block active sites of the catalyst, so it reduces the catalytic activity. Production of 1D nanofibers has been attractive for researchers recently due to their lower affinity to agglomerate, high specific surface, good thermal stability, and high porosity. Catalysts make more active catalytic sites in nanofibers and provide active morphological properties, resulting in active interaction with the reactive molecules due to the small size and interconnected pores. A high specific surface resulted in high dispersion of catalysts embedded in the polymer matrix [35].

PVDF-Pt-Pd/RGO- CeO_2 composite nanofiber (decomposition at 490°C) exhibited better thermal stability than PVDF nanofiber. A significant weight loss was observed for composite nanofiber (55.95wt%) and PVDF nanofiber (51.6wt%) at the temperature range of $460\text{--}500^\circ\text{C}$. The residual amount of composite nanofiber was calculated as 23.13wt% that remarkably larger than PVDF nanofiber (0.042wt%) due to the presence of PtePd and CeO_2 nanoparticles on the PVDF nanofiber [40].

Despite the advantages of PVDF and their derivatives for the purification of water, they suffer from bacteria migration due to their high porosity and surface roughness, resulting in the formation of constant layers. Agglomeration of bio layers includes bacteria and extracellular polymeric materials that they make a bio-pollution that is water permeable and reduces the efficiency of water purification systems based on webs, so many methods for engineering the resistance in front of bacteria pollution of fluoropolymer nanofibers for water purification have discovered. One way is applying antibacterial agents such as silver nanoparticles in or on the nanofibers. These nanoparticles have good antibacterial activity for a wide range of bacterias which are related to silver ions that destroy the cell membrane of bacterias and overcomes the membrane activity of enzymes. Discussion is on the strong keeping of silver nanoparticles in the nanofiber matrix by physical blending. This is due to the excitation of Ag^+ ions in the aqueous media of the nanofiber matrix, and this antibacterial ability continues for 48 hours [4].

An alternative method for surface adhesion resistance of bacteria is the engineering of nanofibers surface by hydrophilic modifiers such as poly (ethylene glycol), poly (vinyl alcohol), and zwitterionic molecules. Among them, zwitterionics have groups of phosphocreatine, sulfobetaine, and carboxy betaine, a promising group of materials to use in the new generation of bacteria anti-adhesions due to comparable operation of them with other works and, in some cases, better than hydrophilic modifiers. Their mechanism is unknown; a neutral charge of zwitterionics absorbs more water molecules due to the high degree of hydrolyzation of the surface that belongs to the reduction of bacterial adhesion. Among different zwitterionic monomers, sulfobetaine methacrylate (SBMA) has advantages because of its ability to more polymerization and copolymerization compared to others. Different surface

modifications such as chemical, plasma, radiation, and flame-retardants exist for designing the surface of fluoropolymers with SBMA (bacteria resistance agents) [4].

Two kinds of nanofibers are used in a membrane to utilize both anti-bacterial and bacterial anti-adhesion to limit bio-pollution of the membrane. For stabilizing silver nanoparticles on PVDF-HFP nanofibers and blending SBMA molecules in polymeric structure for stable exposure to water, electrospinning of two polymers was used to gather them randomly together. By copolymerization of SBMA with methacryl polyhedral oligomeric silsesquioxane (MPOSS), a nonvolatile and environmentally safe organic compound resulted. The presence of PMMA made better spinning ability and formation of even fibers. Results showed that the membrane under positive and negative warm bacterial strains for five days reduced the bacterial surface adhesion (90%) that was comparable with other membranes [4].

Combustion is a process that includes both fluid mechanics and chemical reactions simultaneously. Low attention was paid to the improvement of heat and the weight transfer rate of Ems recently. A metastable intermixed composite (MIC) based on Al by energetic metal-organic frameworks (EMOF) with high specific surface area as reactive. Results showed that MIC increased the released heat a lot (3464J/g). Combustion rate (more than five times faster than mechanical mixed one) and efficiency improved. Also, the decomposition of EMOF could produce lots of gas on the surface layer that avoids cooking and pores formation. These pores are new channels for further chemical synthesis reaction and improved output energy a lot [41].

Lots of anodic materials have been prepared, and their behavior in lithium-ion capacitors (LIC) is important for reducing non-balance power capacity between electrodes because it has an effective role in the cyclic operation of LICs. Highly porous leaf-vein-like MnO_2 @PVDF/TBAC nanofibers were prepared to improve ion conductivity of matrix and cyclic process. MnO_2 as a nanofiber shell improved the cyclic process and avoided fast ion transfer between two electrodes. The nanofibers had excellent thermal stability (to 170°C), 73% porosity, and good ion conductivity ($2.95 \times 10^{-3} \text{ S/cm}$). The resulted LIC had a specific surface of 19.5F/g, a good rate, special cyclic stability (67.2% capacity after 1000 cycles remained), and high columbic efficiency (near 100%) [42].

Giant growth in the internet of things industry indicates the increasing need for the human to it. Among many technologies suggested for non-visible communication, the electronic textile is considerable because of its benefits has application in human health control. To overcome rigid electronics, smart textronics is useful. In this field, nanomaterials such as nanoparticles, CNTs, and graphene are considerable due to their small sizes [6].

Capacitive strain sensor fabric resulted from the dielectric fabric of PVDF-HFP and conductive PVDF-HFP/SWCNT fabric. The gauge factor of it was 130, and it had excellent mechanical properties. The resulted morphology was appropriate for superhydrophobic fabric and better thermal and electrical conductivity that they are good for wearable heaters and heat waste screens [6].

Chargeable lithium-ion batteries have increasing attention for electronic devices and electronic vehicles. In addition to increasing energy density of lithium batteries is limited because of safety problems due to the formation of unusual lithium sediment during repetitive charge/discharge, which causes lithium dendrite formation that has combustion/explosion risk. Solid electrolytes are promising alternatives for liquid ones due to their excellent mechanical properties (good for under pressure, cleaning uneven sediment of Li, and delay the formation of dendrite) and wide electrochemical stability. In addition to nonorganic ceramic solid electrolytes, polymeric ones are interesting too. Polymers like PVDF mix with Li salts but their low ion conductivity is a problem, so approaches like crosslinking, using two block copolymers, usual plasticizers, and adding ceramic fillers are given [43].

PVDF-HFP/LiTFSI/LLZO electrolyte prepared, and presence of 10wt% LIZO nanofiber in it helped the ion conductivity that was due to designing continuous transfer paths for Li-ions. This electrolyte had excellent mechanical properties that resulted in stopping lithium dendrite growth. It had a good electrochemical range (5.2V vs. Li/Li⁺), profitable cyclic operation, and rate [43].

Designing separators resistant to high temperature has an increased delivery ability, and high charge/discharge is necessary for high-performance lithium-ion batteries. Melt electrospun PVDF nanofibers followed by magneto sputtering prepared (Al₂O₃/SiO₂/PVDF, Al₂O₃/PVDF, and SiO₂/PVDF). Among them, Al₂O₃/SiO₂/PVDF had excellent thermal stability (without shrinkage up to 130°C and destroyed in 445°C) and 340% electrolyte uptake. The presence of β phase and polar ceramic nanoparticles gave high conductivity eight times higher than commercial PE. These webs had good discharge (161.5 mAh/g), rate after 100 cycles (84.3%), capacitive in high intensity was 8C (49.8% better than commercial web) [9].

Photodegradation of rhodamine B PVDF/TiO₂ (0-20wt%) under visible light investigated. In 20wt% 80% of degradation in 6 hours under 546nm resulted. The color changed from red to orange, then to yellow, and finally to colorless yellow (complete degradation) by degradation of pollutants. For estimating the degradation rate, the reaction constant was calculated [2].

A tree-like web of helical like PVDF/MWCNT nanofibers followed by hydrothermal growth of MnO_x (these increased specific surface area) used for dye degradation under natural sunlight radiation. This catalyst had an excellent activity for various dyes under sunlight and even darkness [44]. Table 7 gives a comparison of the reaction rate constants of some works.

Table 7 Comparison of the reaction rate constants of some works [44]. Reproduced from [5155621030868], with permission from [Journal of Alloys and Compounds].

Catalyst	Irradiation source	Degradation time (min)	The reaction rate constant (k, min ⁻¹)
MnO _x @PVDF/MWCNTs	Sunlight	20	0.17
Mn ₃ O ₄ -MnO ₂	Visible light	60	0.0456
HNTs/δ-MnO ₂	Sunlight	60	0.05526
Mn ₃ O ₄ nanoparticles	UV	25	0.0757
Co-doped α-MnO ₂ nanowires	Room light	30	0.122

Materials with photothermal ability are fascinating due to using light energy. (GO)/Bi₂S₃-PVDF/TPU nanofibers with (GO)/Bi₂S₃ part as photothermal part prepared. The maximum light absorption of the web was about 90% in 400-2500nm. In the 300s, temperature changing due to the radiation was too fast and intense, and the equilibrium was 81°C [45].

In the PVDF/CNT membrane due to the presence of interfacial polarization due to the piezoelectric CNT improved. High specific surface made lots of sites for sound waves contact. It resulted in more sound absorption in the medium frequency region with a vibration/friction mechanism. Without CNT, the absorption resulted in a low-frequency region. Results showed that acoustic foam with PVDF coverage is a good sound absorber in low to medium frequencies [46].

Electrospun PVDF tree-like nanofiber web prepared. Results showed that this morphology reduced the pore size, narrowed the range of pore size distribution, and dramatically enhanced the specific surface area, so it had excellent

filtration performance. The filtration efficiency with the basis weight of 1 g/m² to 0.26 µm NaCl particles was (almost 100%), and the pressure drop was 124.2 Pa which was comparable to the ultra-low penetration air filters [47].

PVDF nanogenerators

Polyvinylidene fluoride (PVDF) is a piezoelectric polymer with cheap, high mechanical, and excellent piezoelectric properties. Piezoelectric properties correspond to the presence of the β phase in PVDF, which increases by processes like electrospinning (ES). One of its applications is in sound nanogenerators which convert sound to electricity by piezoelectric effect and have applications in microphones and earphones. Parameters such as nanofiber production method, layer properties, polymer or copolymer, surface area, testing conditions, and polymer composite are effective for nanogenerator outputs. This review attempts to scientifically review PVDF sound nanogenerators, enhancing their results, and studying how to apply the electrode. The best kind of electrode wants to enhance its outputs. Among fiber synthesizing methods, the focus is on electrospinning because of its advantages compares to other methods. In-situ synthesis of Ni nanoparticles introduces as the best way to applying the electrode according to studies. It is the best in stability, cost, corrosion, and conductivity. To enhance electrical current output, the interdigitated electrode is the best of all. Results of this review are useful for investigating the effect of electrode applying method, kind of the electrode, and adding additives to nanofibers.

Electronic textiles are important subjects in recent years, which many articles on this subject have been published. In this review, the regard is on the piezoelectric nanogenerators that are sound to electricity converters. In following importance and place of this subject and its significance is discussed.

Electrospun nonwovens, due to their advantages, have application in many fields [4]. Other methods like centrifuge spinning [5], solution blow spinning [6], and so on have developed recently because electrospinning needs high voltage and, in most cases, toxic solvents [5]. Mesoporous nanofibers increase the nanofibers' specific surface area [7] that can enhance properties, especially sensor sensing.

Today, small, environment-friendly, and flexible electrical energy suppliers are a challenge. A way for that is using suppliers with Thermo/pyroelectric [48], piezoelectric [49], triboelectric [49], and dielectric [50] properties. For energy conversion, many research works have been done that have used body movements [49], breath [48], wind blow [48], sound [51], and water pressure [49].

In the following, acoustic, the electrode applying method, piezoelectric nanogenerators, and output enhancing methods are discussed.

Acoustic

Acoustic is studying of mechanical waves in gases, liquids, and solids. Acoustic devices have been developed in phone communication, ultrasound medical tests, human and computer interaction systems, and other fields. Sound waves have sound pressure, frequency, speed, and direction [51].

Metals and semiconductors are used in acoustic devices, but for high-efficiency flexible applications, nanomaterials (such as CNT, graphene, and metal nanowires) are good because of their flexibility, wearing, and sporting ability, and usable underwater [51]. Piezoelectric materials like PVDF have been used in acoustic devices recently, and their best structures in this field are electrospun nanofibers which can sense sound from low to medium frequency. PVDF nanofiber is the bests for wearable sound nanogenerators, which were introduced by Lang and coworkers for the first time [20]. PVDF film could detect sound, but it had a lower piezoelectric effect [22].

Studying sound includes producing, propagation, receiving, and vibration. A sound producible nanogenerator under alternative light or electrical current (AC) or coupling AC with direct electrical current (DC) produce heat which makes periodic temperature changes in surrounding air than by contraction and expansion of the air the sound produces (this is a photo or thermoacoustic model). After propagation of the sound, sound detectors detect it and can produce electricity with piezoelectric effect in piezoelectric sound detectors, and the produced signal can send to the processor [51].

Some flexible and transparent generators, such as the ones based on single-layer graphene or CNT, can use as loudspeakers for LCDs and touchable plans for replaying sounds and images [51].

In 2018 transparent and conductive hybrid nanofilms of orthogonal silver nanowires were used as microphones and loudspeakers [52].

Attention, converting sound to electricity and vice versa is a phenomenon in nanoscale due to the spin conventions in this scale. Spin is an intermediary of different energy conversions like mechanical (like sound), electrical, thermal, and light to each other [53, 54].

Earlier microphones were liquid-based or carbon-based, but they did not have enough quality, so the next generation of microphones has come. They are in 3 categories, including dynamic, piezoelectric, and condenser ones. Old microphones were from metals and semiconductors, which were not flexible and stretchable, so nanomaterial came into the scene [51].

In front of stretch, physical properties (like resistance, current, and voltage) of sound detectors change. For example, as a high-sensitivity strain sensor with a wide range of sensitivity, graphene could detect human throat movements. Still, its very low sensing rang lower than 0.1% could only detect low sound [55]. Graphene can be used as a component in graphene/PVDF nanofiber that could increase sound absorption, compare to PVDF nanofibers by increasing specific surface area between sound and nanofiber, absorption increased in the medium frequency region by increasing friction of sound with PVDF. This composite can decrease absorbent frequency due to the reinforcement of PVDF with graphene [51].

Today, challenges in acoustic nanomaterials are producing them with enhanced specific surface area and conductivity and lower costs, so new methods like 3D printing come into the scene. Also, increasing new acoustic nanomaterials like black phosphor is a challenge too. Another case study is based on the response time and stability of the sound detectors. These acoustic devices with a flexible and biocompatible substrate can attach to human skin as earphones, microphones (like a smartwatch), and artificial throats [51].

Integrating a microprocessor in an artificial throat is a challenge because, after sound sensing, this microprocessor controls the artificial throat to propagate sound [51, 55].

Park and coworkers in 2011, for the first time, used PVDF film as a microphone for cochlea planting [56], and later used by Park and coworkers [57], but a better one is to remove the planting step and use Ghafari Bohloli’s audio wristlet [58]. Table 8 gives some examples of acoustic devices.

Table 8 Some examples of acoustic devices.

device	Structure	operation	application	source
earphone	A rectangular film with	Produce sound from received sound		[51]

	electrodes on the sidelines			
microphone		Converting sound to electricity	Smart devices	[51]
microphone	film PVDF	Converting sound to electricity	Cochlear implantation	,56] [57]
loudspeaker	P(VDF-TrFE) Film with screen printed PSS :PEDOT aqueous ink electrode	Converting electricity to sound (up to 90dB and by two loudspeakers array up to 96dB)		[59]
loudspeaker	PVDF film	70dB	loudspeaker	[60]
The first microphone from the nanogenerator	ZnO piezoelectric nanowires	Converting sound to electricity	Mobile charging during conversation and sound insulation walls near highways and using the sound of passing vehicles	[61]
Microphone and loudspeaker	G/P(VDF-G)/(TrFE multilayer film	Converting sound to electricity with output voltage and current density 3V and 0.37 $\mu\text{A}/\text{cm}^2$ respectively and vice versa		[62]

The first multifunctional acoustic nanodevice	Produced graphene from polyimide and reduced with laser	Converting sound to electricity and then produce sound by helping a microprocessor	Artificial throat	,51] [55]
Strain sensor and loudspeaker	Laser reduced graphene and PVA substrate	Strain sensor and producing sound with the thermoacoustic effect	Artificial throat	[63]

Researches are focus on nanomaterials and nanotechnology to develop an acoustic device with new mechanisms like thermoacoustic sound generators based on graphene, CNT, silver nanowires, and ITO due to high transparency, low thermal capacity, flexibility, a wide range of frequency, expensive, low performance and complicated producing process. Piezoelectric sound detectors have a low performance for detecting throat movements. Piezo-resistant materials for detecting sound encapsulate in PDMS or ecoflex, so they can't release heat in the air and be loudspeakers because their sensitivity for sound is low. For the first time, an artificial throat can be as a microphone and loudspeaker, and this was due to the special pores in the graphene, which help the loudspeaker to detect sound despite other graphene loudspeakers [55]. Like this work, Wei and coworkers produce artificial throat, but they use graphene layers one as a microphone and one as a loudspeaker, and PVA substrate is used to help the device's flexibility [63].

In 2017 effect of a kind of electrode for sound detectors of PVDF film was investigated. Al or Ag sputtered and graphene from CVD used as electrodes and produced pick-to-pick voltage of 9.1V under 2.18MPa tension and 7.6V under 1.75MPa, respectively [22].

Ferroelectric composite PVDF/rGO film could have higher piezo/Ferro/pyroelectric properties than PVDF film [64].

Therefore, maybe PVDF/G nanofiber can produce and detect sound in one device. PVDF can detect noise, but graphene can detect lower sounds, so they can not disturb each other's work. Up to now, sound production from PVDF nanofibers has not been reported.

Electrode applying

For electrode applying conductive materials use, so we first explain them.

Conductive material with enough conductivity, mechanical properties, safety, and stability that does not affect textiles' operation is essential [65]. Table 9 compare different conductive materials.

In recent years nanostructures of metal derivatives with small sizes like nanosheet/particle/wire have been attractive in wearable electronics. They have good banding with a textile substrate,

although their high specific surface can enhance energy and surface tension. Sputtering, electroless plating, and screen printing are the method to apply them on or in textiles [65].

CNT and G are attractive for researchers in wearable electronics. Still, low dispersion of them due to their nonpolar nature is a limitation but GO, due to oxygen groups on its surface can dissolve easily in polar solvents such as water and ethanol. By chemical or mechanical reduction, their conductivity enhances [65]. Graphene, due to its fast temperature gradient because of special flexibility, high thermal conductivity, and very thin thickness, are good for piezo/pyroelectric nanogenerators.

The best way to overcome these limitations is to use hybrid electrodes that combine two or more conductive materials to have the advantages of each material in one electrode [65, 66].

Table 9 Gives a comparison of different kinds of conductive materials [65]. Reproduced from [5155621227281], with permission from [Advanced Materials].

category	examples	advantages	disadvantages
Metals and their derivatives	,semi-conductor ,alloy ,Metal nanoparticles/wires/sheets	Using a lot in high ,engineering high ,conductivity mechanical high ,properties recovery ,stability ,world access ,ability and simple process	low ,Incompatible ease of ,flexibility oxidation and high ,corrosion ,weight and volume and low production
Conductive polymers	,PANi ,PSS/PEDOT :PEDOT and pp ,Pfu ,PPV ,Pac ,Ppy	low ,High flexibility solution ,weight ease ,processability corrosion- ,of control and ,resistant excellent mechanical and optical properties	,Relatively high cost variety of low ,production and ,conductivity stability
Carbon fillers	carbon particle or ,Carbon black carbon ,CNT ,fiber ,carbon aerogel ,micro/nanofiber and G/GO/rGO	,High aspect ratio ,nanoporous structure special mechanical high ,properties electrical and thermal and ,conductivity ambient stability	Difficult structure control and low dispersion

Liquid electrodes	Liquid metals like EgaIn and liquid electrolytes like NaCl	high electrical ,Soft and thermal ,conductivity ,stretchability and ,flexibility flowability	,oxidation ,Heavy ,toxic ,expensive and leakage
-------------------	--	--	---

Wu and coworkers divided stretchable electrode material into three groups [66] as in table 10.

Table 11 gives the method for applying electrodes. However, due to different curve structures, non-even surface morphologies, and complications of materials properties, a good combination between conductive materials and textile systems is difficult [65].

Table 10 electrode examples.

Electrode category	Electrode	conductivity	explanation	source
based on CNT	in PDMS SWCNT	2000S/cm ⁻¹	the ,High transparency mechanical strength of and good ,350Mpa elasticity	[66]
Based on Ag nanowires	Ag nanowires on the surface of the PDMS layer	8310S/cm ⁻¹		[66]
hybrid electrode	Graphene and Ag nanowires	33Ω ⁻¹ (small change after stretch)	94% transparency and 100% stretchability	[66]
Based on graphene	Graphene (CVD)	Allow to simultaneous charge transfer of diffusion nets	8μA/cm ⁻² under .8V and 0 0.083-0.271 bending stretch	[66]

Based on Ag nanowires	Dip coating by Ag nanowires (prepared by solvothermal) dispersed in ethyl alcohol		electricity production by the piezoelectric effect of PVDF film and sound production by Ag nanowires	[67]
Based on graphene	Screen printing of graphene ink		Enhancing pyroelectric effect of PVDF film (under IR radiation) due to high thermal and electrical conductivity	[69]

Table 11 different electrode applying methods [65]. Reproduced from [5155621227281], with permission from [Advanced Materials].

methods	categories	advantages	disadvantages
coating	casting	and for every ,fast ,Simple size and both sides coating	using a lot of ,Time-consuming solution and low mechanical properties
	plating	The most simple method for high ,film formation and cheap ,efficiency	Uncontrollable thickness
	Doctor blading	The accurate thickness and low waste	Relatively low speed and for the solution with high crystallinity percent
	Spin coating	and ,even ,Simple reprocessing	Surface coating without any pattern

methods	categories	advantages	disadvantages
Spinning (the main method for yarn or fiber production)	Wet spinning	High mechanical operation	Low conductivity and speed and need solvents
	Dry spinning	a great ,Fast solidification and ,variety of raw materials application	need solvents with high volatility
	Melt-spinning	high speed ,cheap ,Simple and no ,and no solvents danger to the environment	,Needing high temperature ,difficult to produce fine fibers needing polymer with melting and needing special ,ability machinery
	electrospinning	,high aspect ratio ,Easy and ,controllable pore size special mechanical properties	Needing high voltage and for the small area
plating	Electroless plating	High conductivity	,Low performance and stability and time- ,high production limit consuming
	Thermal deposition	Hard, anti-corrosion, stable, and scratch-resistant	Needing lots of space
	sputtering	,High speed and production even and better adhesion	High cost and low target utilization rate
Printing (for high production and reduce surface complications)	Fused deposition modeling	high speed and ,Cheap simple	,Low mechanical properties and ,layer-by-layer appearance low quality
	Screen printing	simple, easy, and not expensive	Limitation for a solution with high viscosity and low volatility
	Inkjet printing	High accuracy	Not high speed
	Roll-to-roll printing	For high production and complication of structure and pattern	Needing process with constant slower and higher cost ,pressure
intrusion	Liquid intrusion	Very flexible and stretchable	Just for liquid electrodes and ease of leakage

Flow coating is for one side coating or coating different sides with different coatings. Spin coating is for devices with symmetrical and almost smooth shapes. Both of them have limitations for

devices with a hole, bulge, or surface irregularity but roll coating widely uses for applying a thin layer on different substrates. However, this method is not for low production and curved shapes [65].

Gel-spinning is a kind of spinning method which uses a soft gel to achieve high strength or other unique properties [65].

In plating, the surface is coated with one metal. In electroplating, the metal is on the anode, and the material is on the cathode. Both of them are floating and connected with an electrolyte solution, including metal salts or dissolved ions. They are connected to an external power source to produce an electrical current, which transfers metal ions to the cathode. In electroless plating, an electrical field is not required, and according to redox interaction, metal ions in the chemical bath with a strong reducer reduce to metal and then deposit on the surface of the material with any geometry and complicated shape [65].

Other printing methods are gravure printing, flexographic printing, and offset printing. Moreover, printing with low raw material can produce a lot of output, reducing the costs a lot. This method is a cost-effective one for making electrical systems on a large scale [65].

Conductive materials can place in/out of material or can blend with it homogeneously or by spiral cladding can apply to them [65].

Conductive fabrics can achieve by in-situ synthesis, which is a kind of electroless plating, and by the in-situ synthesis of nanoparticles, the cost reduces. In table 12, some examples of electrode applying are written.

From comparing three articles of in-situ synthesis according to table 12 by compositing graphene and silver [69] instead of graphene alone [70], the electrical resistance reduced (from 35.7 Ω .cm to 3.8 Ω .cm and 9.3 times higher conductivity than graphene) and by copper nanoparticles reached 0.5 Ω .cm (7.6 times higher conductivity than graphene and silver composite), so the presence of metal can enhance conductivity. Therefore, composting is an effective way to achieve advantages of both metal and graphene that is following the results of source number 67.

One of the problems of metals is corrosion. Gold and platinum are noble metals, but they are expensive, and copper with low cost has high corrosion ability, so the best one is nickel, the anti-corrosion agent of stainless steel that has a reasonable price. In some cases, the coating of nickel is applying to the copper. Then nano/micro-roughness is used to enhance anti-corrosion by making a superhydrophobic surface [71]. In another work, it used a coating of graphene to improve electrical conductivity anti-corrosion of stainless steel [72]. Self-healing nanofibers coating or other anti-corrosion coatings can use too. Some examples of different electrodes are presented in table 12.

Table 12 examples of electrodes.

electrode	substrate	Electrode applying method	Electrode conductivity	source
Silver glue ink on the substrate of PET	Electrospun PVDF	Inkjet printing with interdigitated pattern		[73]
SWCNT/PVDF-HFP nonwoven	solution blown PVDF-HFP	Solution blow spinning with $W_{\text{SWCNT}}/W_{\text{PVdF}}=0.6$	3.1k Ω /sq	[6]
GO and GO/Ag solutions	fabric PET	In-situ synthesis with heat and hydrazine	0.26 S/cm	[69]
rGO	fabric PET	In-situ ⁺ synthesis of sn^4 as cross-linking agent and ⁺ and sn^2 reducer	0.028 S/cm	[70]
Copper nanoparticles	fabric PET	click electroless plating of copper acetate salt and hydrazine	0.5 Ω .cm	[74]

Piezoelectric materials

In 1880, Pierre Curie and Jacques saw a phenomenon when studying the quartz crystal properties. Under force, a wafer that produced positive and negative charges on the electrode on the wafer's

surface and by removing the pressure the charges disappeared, this is piezoelectric effect. Many of the materials like ceramics, composites, and polymers have these properties [51].

Comparison of piezoelectric materials

Piezoelectric materials are divided into two groups piezoceramics and piezopolymers. Between piezopolymers, PVDF is a semicrystalline polymer with five different crystalline phases. Among them, the β phase has high importance in high polarization and piezoelectric sensitivity, increasing this phase is important. PVDF-TrFE has advantages comparing to PVDF, including ferroelectric property, actual Curie transition temperature, and high electromechanical coupling coefficient. Due to flexibility, ease of the process, good chemical resistance, excellent biocompatibility, and mechanical strength, these two polymers have been widely used in piezoelectric textiles [65].

A comparison of piezoceramics and piezopolymers is presented in table 13. Piezoceramics have a higher piezoelectric constant but lower flexibility compares to piezopolymers, so one way can be using them in a hybrid material. Although both of them can have nanowire/fiber/tube/sheet structure and due to nanostructure, the piezoelectric effect, flexibility, mechanical properties, and sensitivity enhance [65].

According to table 14, it seems that finding an alternative for PVDF has been critical in recent years. Maybe a new way is melt-electrospinning PP because solution electrospinning of it due to not having a solvent is impossible. One limitation of melt electrospinning is its higher diameter [75], which can be solved by adding additives such as NaCl that can reduce the diameter to 400nm [76] and then solve the salt porous nanofibers achieve which is another way to enhance the output. Also, the electrospinning of PLLA is promising too, but this polymer's solvent is more dangerous than PVDF, so the melt electrospinning of this polymer is more common.

Table 13 comparing piezopolymers and piezoceramics [65]. Reproduced from [5155621227281], with permission from [Advanced Materials].

category	Main types	advantages	disadvantages
piezoceramics	ZnO, PZT, BaTiO ₃ , PbTiO ₃ , KNbO ₃ , LiNbO ₃ , LiTaO ₃ , Na ₂ WO ₃ , GaN, CdS, InN, PbZrO ₃ , ZnS	Higher piezoelectric constant, special energy conversion efficiency, and high strength	Mechanically brittle, heavyweight, poisonous, low durability

piezopolymers	PVDF and its polymer PVDF-TrFE, PA-11, PP	Inherently flexible, easy for processing, adequate mechanically strong, a strong sensitivity	Inherently flexible, easy for processing, adequate mechanically robust, and intense sensitivity
---------------	--	--	--

Table 14 piezoelectric output of other piezopolymers.

Advantages compare to PVDF	output	Production method	sample	source
Cheaper, higher mechanical properties and chemical resistant	2.8pJ/s	Melt electrospinn ing	PP/MWCNT (0.1wt%)	[77]
	84.0±22.8mV/ N	Foam formation	PP with 2mm thickness	[78]
Likely to PVDF film	0.064V.m/N	Film formation	PLLA film	[79]

Mechanisms of piezoelectric nanogenerators

An easy way for making piezoelectric nanogenerators is a metal/isolator/metal structure including a piezoelectric isolator layer which sandwich between two metal electrodes, so by applying pressure, the ions produce and flow from the outer circuit. After releasing a current with the opposite sign, the resulting current is a conventional AC. Interestingly, if the connected vice versa, the current and voltage reverse [9, 65].

Piezoelectric nanogenerators are divided into three categories:

1. Based on a single fiber
2. Based on fabric which overcomes the number limitation and low specific surface of the first category, so result in a higher output signal
3. Hybrid ones to have higher output.

As a result, nanostructure surface and hybrid piezo-materials are the ways to have higher outputs. Protecting from the effective surface like encapsulating polymer for improving mechanical

properties and stability for piezoelectric nanogenerators with nanostructures is necessary. Different raw materials, conditions (like force, frequency, and contact area), and geometrical size, comparing various works' output is difficult [65].

Increasing current density of nanogenerators

In comparison to triboelectric nanogenerators up to now, piezoelectric nanogenerators had lower outputs. Still, they are more stable in humidity and dust, so increasing their output up to triboelectric nanogenerator's outputs can be the most powerful microscale power sources [80].

From the invention of the first piezoelectric nanogenerators made from ZnO nanowires in 2006 which deformed by the tip of AFM, many kinds of research have been done to increase their output voltage to hundreds of volts which is enough to power most electronic devices of human daily uses but the current output still is small that is a limitation for developing piezoelectric nanogenerators [80]. Methods to increase the current output of piezoelectric nanogenerators are listed in table 15.

According to the merits of PVDF, this polymer has been studied more. In the following investigating of PVDF, nanofiber formation is the aim by focusing on electrospinning. But recently, other methods like solution blown spinning (which uses compact air force to thin the jet) [6] and melt electrospinning [84] have been developed due to limitations of electrospinning (requiring high voltage and organic solvents). In 2013 needless electrospinning was used to enhance piezoelectric output, which had the application in cooling textiles [85].

Electrospinning contains four steps:

1. Charging liquid droplet and forming Taylor cone (jet formation);
2. Jet thinning in a straight line;
3. Jet thinning in an electrical field and increasing bending instabilities;
4. Solidification of the jet on the collector in the form of fiber [86].
5. PVDF piezoelectric nanofibers properties investigation
6. Investigating and corporation of PVDF nanofibers have been attractive in recent years, and for improving their properties, doping with different compounds like (small molecules/polymers/nanostructures) is a good way. Although the nanofibers' morphology can change by controlling the production parameters, this is critical to enhancing material properties. For example, nanofiber morphology is effective for piezo/pyro/ferroelectric properties because diameter reduction due to more drawing can increase β phase formation [9].

Table 15 increasing current output methods.

Current density and further information	Layer and electrode	Increasing current output methods	source
Designing the device for radial, vertical and wide integration of nanomaterials	Piezoelectric materials with electrode	Choosing piezoelectric materials with high piezoelectric effects like PVDF, ZnO, GaN, PZT, and BTO	[80]
150 μ A/cm ²	Thin PZT film with interdigitated electrode	interdigitated electrode	[80]
290 μ A/cm ² 1.93) times higher than 150 μ A/cm ² and 1.6 times higher than triboelectric nanogenerators (180 μ A/cm ²))	Sm-PMN-PT NW/PVDF with 3D electrode	3D intercalation electrode (to improve charges surface polarization by formation common interfacial boundaries in the piezoelectric material)	[80]
Improving output	interdigitated electrode (helping to higher volumetric density) for P(VDF-TrFE)	Sandwiching the layer between compton films in the form of wave	[81]
0.079Vm/N sensitivity and higher strength and flexibility from the bulk form and higher piezoelectric effect from PVDF nanofibers	Electrospun PZT nanofibers with interdigitated electrode	interdigitated electrode from Au/Cr to be in line with nanofibers	[82] and similar to [83]

Methods to improve the piezoelectric properties of PVDF include:

1. Electrospinning (drawing and poling Simultaneously) [9]
2. Polymer blending [13]
3. Heat annealing [10]
4. Nanoconfinement [10]
5. PVDF copolymers [10, 20]

- 6. Additive addition BTO [10], Ce^{3+}/G [11], MoS_2 [12], Ag [14], ZnO [15], GS [87], Pt [17], ILS [1] and TiO_2 [9] (by adding additives with negative or positive charges due to negative charge of CF_2 and positive charge of CH_2 , nucleating the β phase increases [19]).
- 7. Increasing the specific surface area
- 8. Hybrid devices
- 9. Device properties like layer thickness.

For investigating the piezoelectric properties, PFM is useful for measuring the piezoelectric constant [10], but nanofiber diameter and crystallinity information is helpful. FESEM can give nanofibers diameter. XRD provides the crystallinity percent of each phase of PVDF [59], and FTIR shows that which phases [15] and materials are present in PVDF. But the best way is to measure the piezoelectric outputs directly by applying pressure (sound/wind/weight pressure) to the sample.

For increasing the output of piezoelectric nanogenerators, enhancing the β phase content is a way investigated in previous sections but in the following other methods introduce too. Then a review of PVDF nanofibers acoustic nanogenerators enhancing output methods is the subject. This enhancement is significant for practical applications.

Increasing specific surface area methods

Increasing specific surface areas can achieve with the methods that include porous nanofibers, penetrated electrodes, and nanostructures forming on the surface by plasma treatment. Increasing specific surface area can achieve with Altera thin nanofibers too but up to now, no one has investigated this way. Signs of these nanofibers are in SEM images of nanofibers of source number 2 which can investigate their effect in further studies.

Many physical and chemical modifying electrospun nanofibers exist for achieving porosity and pore size. Usually, electrospun nanofibers have a solid structure, but if pores form in/on them, the specific surface area increases a lot [88]. Nanofibers porosity is controllable with changing density, size, form, and pores distribution [86]. Thermal treatment also can make porous structures in carbon fibers and ceramic fibers by removing one part [89]. In table 16, different porosity formation methods are listed.

Table 16 pore formation methods in/on nanofibers.

Method explanation	Porosity formation method	source
jet partially fast freezing by fast evaporating of very volatile solvent or collecting nanofibers in the liquid bath	Phase separation between polymer and solvent	[86]

Method explanation	Porosity formation method	source
Vapor phase separation (usually, with electrospinning in high humidity, the water molecules in the air works as nonsolvent) and liquid phase separation	Phase separation between polymer and nonsolvent	[90]
Jet with triple-phase separation due to difference between volatility of solvent and nonsolvent (by changing ratios of this system) and pores form by changing relative rates of solvent/nonsolvent, controlling of phase separation dynamic	Phase separation of the liquid section in polymer, nonsolvent, and solvent system	[91]
Phase separation between polymer and nonsolvent due to residual solvent in nanofiber by receiving nanofibers to nonsolvent bath and pore formation due to miscibility between solvent and nonsolvent	Collecting the nanofibers in a nonsolvent bath	[91]
Washing small molecules (like salt), block copolymers, polymers from nanofibers, or calcinating (the best way because pores formation by solvent evaporating is time-consuming and sometimes is impossible to remove one phase completely)	Selective removal of one phase of nanofiber	[86]
Controlling porosity by adjusting the ratio of two phases in nanofibers	Thermal degradation of one phase	[89]

In table 17, examples of other increasing specific surface area methods (plasma and hybrid devices) are listed.

Table 17 plasma and hybrid devices as methods to increase the output.

Output after applying the method	First output	Method explanation	Increasing output method	layer	source
For a layer with 45% porosity 21V and 21.1 μ A	For its film 2-3V	Using phase separation diagram	Porous nanofibers	Electrospun P(VDF-TrFE)/DMF (solvent)/water(non-solvent)	[18]
3 times higher piezoelectric coefficient and 0.6 μ W/cm ²			Porous nanofibers	Electrospun nanofibers in 60% relative humidity and negative voltage polarization	[92]
1V increased		Cactus like morphology and super hydrophobic	Porous nanofibers	Electrospun nanofibers in 62% relative humidity	[93]
25.6nA and 118pC	12.5nA and 34.8pC	Increasing contact and conductive ways and superhydrophobic layer	Penetrated electrode (O ₂ plasma)	Electrospun BTO/P(VDF-TrFE) by the sandwiched electrode and encapsulating in PI tape	[10]
Increasing a lot		Increasing adhesion between electrode and layer	Plasma treatment	Electrospun PVDF	[94]
25V, 98.756 μ W and 1.98 mW/cm ³	Piezoelectric output was 2.5V, 9.74 μ W, and	Combining piezoelectric and triboelectric effects	Hybrid device	P(VDF-TrFE) with Ag upper electrode and PDMS/MWCNT film lower electrode	[49]

Output after applying the method	First output	Method explanation	Increasing output method	layer	source
	0.689 mW/cm ³				

Layer's properties such as thickness, nanofiber diameter, bead presence, web area, presence of hole(s) on the electrode to increase the contact of sound with layer and polymer type effect on piezoelectric output.

In 2015, the effect of electrospinning parameters and polymer solution concentration on increasing the β phase content and electrical output was investigated. The β phase content rises by reducing nanofiber diameter, and there is an optimum thickness for the layer to get the best result [95].

Lang and coworkers in 2016 have electrospun PVDF nanofibers. The optimum diameter was achieved because low diameters had beads and high ones caused lower outputs. The resulted layer is sandwiched between two gold-sputtered PET films with five times higher sensitivity than PVDF film. In 320Hz with 115dB, 3.1V received and above 100Db remove noise. In 60-90Db, the output was 1.2-245mV. Forming a hole in the middle of the electrode and increasing the web area resulted in higher sensitivity. By increasing the thickness up to optimum thickness, this trend saw too as well as for increasing nanofibers alignment, nanofiber diameter reduction, and using copolymers (for P(VDF-TrFE) 750mV/Pa in 100dB) [20].

In this group's next work, increasing the numbers of the holes caused higher outputs, and they proved that using this nanogenerator avoids corrosion in stainless steel in the process [96].

Another way to increase the nanogenerator's output is to place it on the curved shape surface (in the form of half-cylinder), which causes increasing the surface area and this increasing dependence on radius and cylinder angle investigated for PVDF film [97].

Bending layer of PVDF nanofiber under 70° with only one electrode (with the advantage of do not have short circuit problem) of ion sputtered which encapsulated in Al foil used for thief-catcher [98], so we can conclude that maybe bending nanofibers is a way to increase the output.

Acoustic nanogenerators increasing output methods

In 2016 electrospun PVDF/MoS₂ nanofibers were prepared, and the diameter compared to PVDF nanofibers decreased. By decreasing the diameter, crystallinity, strength, mechanical properties, and piezoelectric effect increased. The presence of nanosheets by decreasing α phase nucleating caused higher β phase content. Under 6.6Pa, the output voltage was 2.5V and the layer was sensitive up to 0.61Pa, and under 8.8kPa the voltage was 14V which could turn on 8LEDs. In

90dB, the voltage was 12V, and the open-circuit current was 2nA. The maximum amplitude was in 100-150Hz, and the sensitivity was 19V/Pa. Three capacitors with rectifier bridge circuit with 9V in 44s charged and its power density was 671Mw/m³ but for one capacitor was 671Mw/cm³ [12].

In 2019 Ghafari and coworkers electrospun PVDF nanofibers (a method for increasing the output). PET substrate is used to apply ink. For making a sensor, IDE is used. For depositing Ag electrode Diamtix inkjet printer was used. For the ultrasonic test, a PZT piezoelectric converter and a PVDF layer receiver were used. The resulted nanofiber had a 75% β phase. By reinforcing receiving signal, no giant change in performance saw but was effective for receiving the signal. The performance had an inverse relation. The performance was constant up to 100kHz but decreased, which can be related to not having enough time for recovering the applied strain. The appropriate range for maximum performance was 1-100kHz frequency, the acoustic range, so it can be an acoustic sensor. The ultimate performance was under 40% [71].

In 2016 a method for producing electrospun PVDF/G nanofibers doped by Ce³⁺ was used, which was appropriate for in-situ synthesis of a wide area, high sensitivity, and flexible pressure sensors. The sensor could sense up to 2Pa, and it was very sensitive, which as a nanogenerator could give 11V with 6nA/cm² current density that could immediately turn 10LEDs on. The output power in 1M Ω was 6.8 μ w. The sensor as an acoustic sensor could produce 3V under 88dB. Adding G could nucleate β phase content after drawing and step by step polishing, giving a higher piezoelectric effect. Dehydrated aluminum cerium sulfate is used for doping cerium ions. The β phase content was reached 96% and after adding G reached 99%. Under repeating 8N pressure force in 4Hz and the vertical pressure of 6kPa on the top of the sensor, the output with 1% G reached 11V from 4.5V. For calculating of pressure dividing force on the contact area used. Wind energy with 8m/s speed had 3.2V output [11].

In table 18, comparing sample conditions and works results, is listed.

Table 18 comparing acoustic works. dB for SPL, μ m for web thickness, cm² for web area, mm hole diameter, Hz for frequency, and nm for the nanofiber diameter.

electrode	sample	condition	variables	sensitivity	source
Conductive fabric	PVDF	250 μ m, 9 \times 7.5cm ² , 90dB	PVDF	-	[9]
			TiO ₂ /PVDF	17.5V, 26000V/kPa	

electrode	sample	condition	variables	sensitivity	source
Conductive fabric	PVDF	88dB	PVDF	2380V/kPa	[11]
			G/Ce/ PVDF	3V, 5970V/kPa	
-	PVDF	150 μ m, 11 \times 8.5cm ² , 90dB	PVDF (107 \pm 5nm)	271V/kPa	[12]
			MoS ₂ / PVDF (75 \pm 10nm)	19000V/kPa, 2nA, 12V	
PET nonwoven with sputtered copper/nickel	PVDF	100dB, 315- 1250Hz	PVDF (156 \pm 13nm)	49mV, 24.5V/kPa	[14]
			Ag/ PVDF (169 \pm 21nm)	55.8 mV, 25.9V/kPa	
Inkjet printing of Ag ink	PVDF	86-89dB		100 mV, 210.8V/kPa	[71]
Gold sputtered PET film	PVDF	220Hz	60dB	1.2mV	[20]
			115dB	2.29V	
	PVDF	40 μ m, 220Hz, 115dB	6.4mm	110V/kPa	
			12.8mm	200-225V/kPa	
	PVDF film		No change	42.5V/kPa	
	PVDF			266V/kPa	
	PVDF		No hole	0.5V	
			One hole	2.5V	

electrode	sample	condition	variables	sensitivity	source
	PVDF	12.8mm, 220Hz, 115dB	20 μ m	161V/kPa	
			40 μ m	205V/kPa	
	PVDF	40 μ m, 12.8mm, 220Hz, 115 dB	2cm ²	50V/kPa	
			12cm ²	200-225V/kPa	
	PVDF-TrFE	100 dB		1.5V, 750 V/kPa	
Gold sputtered PET film	PVDF, 3 \times 4cm ² , 20 μ m, 310 \pm 60nm		One hole	6.6 μ A, 5.3V	[96]
	PVDF-TrFE, 3 \times 4cm ² , 20 μ m, 240 \pm 40nm		One hole	11.2 μ A, 7.8V	
	PVDF-TrFE, 3 \times 4cm ² , 20 μ m, 240 \pm 40nm		Eight holes	28.5 μ A, 14.5V	
Stainless steel mesh and Al foil	PVDF	160Hz, 115dB		75V, 45mA/m ²	[99]
Copper foam and nylon fabric with PEDOT: PSS nanofibers coating	PVDF	125Hz, 110dB, 20 μ m,		523V, 25mA/m ²	[100]
Gold sputtered PET film with 8 holes	PAN, 3 \times 4cm ² , 30 μ m, 215 \pm 50nm, 100-500Hz, 115dB		polymer	58V, 12 μ W/cm ² , 12 μ A	[101]

Sensor sensitivity is calculated from below equation where V is the output voltage, P equals 0.00002Pa, and I_p is the sound pressure [20]. In sources number 100 and 101, the nanogenerators work with triboelectric effect.

$$S = \frac{V}{P} = \frac{V}{10^{-5}} = 10^5 \frac{V}{Pa}$$

According to the above results, the kind of dopant and finding the optimum condition for the sample for testing affects the output. Up to now, the impact of a kind of electrode for nanofiber

web has not been investigated. Still, similar to this for PVDF film showed that the type of electrode could change the output a little [12]. Still, its effect is not a lot (because in all the above works with different electrodes, no big changes were seen in outputs). It seems that the kind of electrode and electrode applying method is essential for lower cost or getting more functions from the layer.

For the first time saw that PAN showed a better piezoelectric effect than PVDF [101], so a new subject for further studies is acoustic sensors based on PAN composite nanofibers.

Future of PVDF nanogenerators

As mentioned earlier, hybrid electrodes are the best, and printing is the best method for electrode applying, so inkjet printing of Ag/G ink is the best solution, but it is expensive, and low dispersion of G is a problem; therefore, its development has limitations [102]. Maybe printing sometimes is hard due to no access to a good printer and makes applying any patterns impossible. Spin coating is a simple and available method, but just like using ink, applying them on a porous nanofiber layer may result in higher output just like penetrated electrodes or may cause a short circuit or maybe do not penetrate in the layer, so a solution is to apply the ink on a PET film but in sound maybe needs to make holes on the layer to make possible for the layer face with sound easier. The Sputtering of nickel is good because of its anti-corrosion, cheapness, and good conductivity. Still, for higher stability and cost efficiency, in-situ synthesis of nickel on layer is the best way (similar to it done for PET fabric [103]) and due to good adhesion of nickel nanoparticles with layer, nowadays is attractive but sputtering is suitable for high productivity and is a dry method. For higher conductivity, using both copper and nickel is away. Sputtering of gold had little outputs and high cost [105]. However, in-situ synthesis of gold with gold chloride and a reductant such as DMF is a way to lower cost [27]. The best way is an in-situ synthesis of nickel on the layer from the above information. In 2011, making PVDF electrospun web conductive in-situ synthesis of Ag was done for cardiography tests [104]. Comparing all these suggestions is a good subject for further articles. Among these electrodes, Ag/G ink can use to produce sound by electrode applying the same source number 69. It seems that in-situ synthesis compares to sputtering should have higher outputs due to more stability and adhesion of this method (dip-coating of graphene showed better results compare to spiral coating for piezoelectric nanogenerators with human hand force [21]) and also both of them should have higher outputs compare to Ag/G ink due to lower conductivity of the ink similar to source number 23. Interdigitated electrode is the best way to increase current density, which can be used in sputtering, printing, and spin coating. The results of this heading are presented in the following table 19.

Table 19 results of future PVDF nanogenerators.

Electrode	merits	demerits
In-situ synthesis of Ni	Low cost, high conductivity, attaching on the layer a cause to higher output	The wet process so needs controlling, and it is harder to apply

Electrode	merits	demerits
Sputtering of Ni	Dry process, high conductivity, easy to apply	High cost, lower attaching with the layer
printed G ink	Low cost, easy to apply, dry process	Lower conductivity
Printed Ag/G ink	easy to apply, dry process, higher conductivity than G ink	Higher cost than G ink
Spin coating of ink	Cheapest and easiest way	Lower accuracy
Interdigitated electrodes	a way of increasing output without depending on the kind of electrode applying method and kind of using the material for the electrode	
Electrodes with the hole on them	A way to increase the output for acoustic nanogenerators	
holed electrodes of printed G ink	Bests for acoustic nanogenerators (suggestion for further works)	Should investigate

Flowchart 1 is introducing the output increasing methods for PVDF nanofibers nanogenerators.

Flowchart 1 introducing output increasing methods for PVDF nanofibres nanogenerators.

output increasing methods	parameters of the layer	layer thickness
		layer area
		nanofiber diameter
electrode		impedance of load
		porous nanofibers
		choosing the best nanofiber material
test's condition (for acoustic nanogenerators)		encapsulating the layer
		electrospinning of the nanofibers
		flexible electrode
		interdigitated electrode
		integrated electrodes
		permeated electrodes
		frequency
		lowering of vibrations
		SPL
		choosing the good way to apply the sound to layer
		holes on the electrode

Conclusions

PVDF-based nanofibers possess increased attention in research and application fields. Lots of articles on the subject of nanofibers of PVDF have been published. This review wants to

summarize and review the growths in this field. This is logical because these materials are the main elements in developing many devices (sensors, fuel cells, photocatalysts, and piezoelectric devices) for future applications. Many research groups combine nanofibers of PVDF with other small molecules, polymers, and nanostructures that these systems have made for modern technology requirements and give new properties by many practical applications.

Conflict of Interest: Author has no conflict of interest relevant to this article and confirm that no other researchers are involved in this manuscript and no potential ethical issue exists.

Sources

- [1] Mahdavi Varposhti, A., et al. (2020). "Enhancement of β -Phase Crystalline Structure and Piezoelectric Properties of Flexible PVDF/Ionic Liquid Surfactant Composite Nanofibers for Potential Application in Sensing and Self-Powering." *Macromolecular Materials and Engineering* **305**(3): 1900796.
- [2] Lou, L., et al. (2019). "Visible light photocatalytic functional TiO₂/PVDF nanofibers for dye pollutant degradation." *Particle & Particle Systems Characterization* **36**(9): 1900091.
- [3] Itankar, S., et al. (2019). Comparative photoluminescent study of PVDF/Eu³⁺ and PEO/Eu³⁺ electrospun nanofibers in photonic fabric. *AIP Conference Proceedings*, AIP Publishing LLC.
- [4] Anand Ganesh, V., et al. (2019). "Engineering silver-zwitterionic composite nanofiber membrane for bacterial fouling resistance." *Journal of Applied Polymer Science* **136**(22): 47580.
- [5] Hernandez, C., et al. (2019). "Performance evaluation of Ce³⁺ doped flexible PVDF fibers for efficient optical pressure sensors." *Sensors and Actuators A: Physical* **298**: 111595.
- [6] Ho, D. H., et al. (2019). "Multifunctional smart textronics with blow-spun nonwoven fabrics." *Advanced Functional Materials* **29**(24): 1900025.
- [7] Ning, J., et al. (2016). "Tailoring the morphologies of PVDF nanofibers by interfacial diffusion during coaxial electrospinning." *Materials & Design* **109**: 264-269.
- [8] Wu, S., et al. (2019). "Ceramic nanoparticle-decorated melt-electrospun PVDF nanofiber membrane with enhanced performance as a Lithium-Ion Battery Separator." *Acs Omega* **4**(15): 16309-16317.
- [9] Alam, M. M., et al. (2018). "Biomechanical and acoustic energy harvesting from TiO₂ nanoparticle modulated PVDF nanofiber made high performance nanogenerator." *ACS Applied Energy Materials* **1**(7): 3103-3112.
- [10] Hu, X., et al. (2019). "Improved Piezoelectric Sensing Performance of P (VDF-TrFE) Nanofibers by Utilizing BTO Nanoparticles and Penetrated Electrodes." *ACS applied materials & interfaces* **11**(7): 7379-7386.

- [11] Garain, S., et al. (2016). "Design of in situ poled Ce³⁺-doped electrospun PVDF/graphene composite nanofibers for fabrication of nanopressure sensor and ultrasensitive acoustic nanogenerator." *ACS applied materials & interfaces* **8**(7): 4532-4540.
- [12] Maity, K., et al. (2017). "Two-Dimensional piezoelectric MoS₂-modulated nanogenerator and nanosensor made of poly (vinylidene Fluoride) nanofiber webs for self-powered electronics and robotics." *Energy Technology* **5**(2): 234-243.
- [13] Sengupta, P., et al. (2020). "A comparative assessment of poly (vinylidene fluoride)/conducting polymer electrospun nanofiber membranes for biomedical applications." *Journal of Applied Polymer Science* **137**(37): 49115.
- [14] Wu, C. and M. Chou (2020). "Acoustic-electric conversion and piezoelectric properties of electrospun polyvinylidene fluoride/silver nanofibrous membranes." *Express Polymer Letters* **14**(2).
- [15] Alam, M. M., et al. (2018). "An effective wind energy harvester of paper ash-mediated rapidly synthesized zno nanoparticle-interfaced electrospun PVDF fiber." *ACS Sustainable Chemistry & Engineering* **6**(1): 292-299.
- [16] Martins, P., et al. (2014). "Electroactive phases of poly (vinylidene fluoride): Determination, processing and applications." *Progress in polymer science* **39**(4): 683-706.
- [17] Ghosh, S. K. and D. Mandal (2018). "Synergistically enhanced piezoelectric output in highly aligned 1D polymer nanofibers integrated all-fiber nanogenerator for wearable nano-tactile sensor." *Nano Energy* **53**: 245-257.
- [18] Abolhasani, M. M., et al. (2019). "Thermodynamic approach to tailor porosity in piezoelectric polymer fibers for application in nanogenerators." *Nano Energy* **62**: 594-600.
- [19] Wan, C. and C. R. Bowen (2017). "Multiscale-structuring of polyvinylidene fluoride for energy harvesting: the impact of molecular-, micro-and macro-structure." *Journal of Materials Chemistry A* **5**(7): 3091-3128.
- [20] Lang, C., et al. (2016). "High-sensitivity acoustic sensors from nanofibre webs." *Nature communications* **7**(1): 1-7.
- [21] Moarref, Z., et al. (2017). Treatment of PVDF/ZnO Electrospun Fibrous Mat with Graphene Oxide Followed by Thermal Reduction to Produce Mechanical to Electrical Converter, Amirkabir University of Technology.
- [22] Park, S., et al. (2017). "Energy harvesting efficiency of piezoelectric polymer film with graphene and metal electrodes." *Scientific reports* **7**(1): 1-8.
- [23] Ponnamm, D., et al. (2020). "Electrospun nanofibers of PVDF-HFP composites containing magnetic nickel ferrite for energy harvesting application." *Materials Chemistry and Physics* **239**: 122257.

- [24] Zheng, T., et al. (2017). "Local probing of magnetoelectric properties of PVDF/Fe₃O₄ electrospun nanofibers by piezoresponse force microscopy." *Nanotechnology* **28**(6): 065707.
- [25] Kaur, G. A., et al. (2020). "Modification of structural and magnetic properties of Co_{0.5}Ni_{0.5}Fe₂O₄ nanoparticles embedded Polyvinylidene Fluoride nanofiber membrane via electrospinning method." *Nano-Structures & Nano-Objects* **22**: 100428.
- [26] Lee, S. H., et al. (2020). "Fabrication and characterization of piezoelectric composite nanofibers based on poly (vinylidene fluoride-co-hexafluoropropylene) and barium titanate nanoparticle." *Fibers and Polymers* **21**(3): 473-479.
- [27] Kushwah, M., et al. (2019). "Dielectric, pyroelectric and polarization behavior of polyvinylidene fluoride (PVDF)-gold nanoparticles (AuNPs) nanocomposites." *Vacuum* **166**: 298-306.
- [28] Mayeen, A., et al. (2020). "Flexible dopamine-functionalized BaTiO₃/BaTiZrO₃/BaZrO₃-PVDF ferroelectric nanofibers for electrical energy storage." *Journal of Alloys and Compounds* **837**: 155492.
- [29] Li, H., et al. (2018). "Enhancing the tactile and near-infrared sensing capabilities of electrospun PVDF nanofibers with the use of gold nanocages." *Journal of Materials Chemistry C* **6**(38): 10263-10269.
- [30] González-Benito, J., et al. (2019). "PVDF based nanocomposites produced by solution blow spinning, structure and morphology induced by the presence of MWCNT and their consequences on some properties." *Colloid and Polymer Science* **297**(7): 1105-1118.
- [31] Lou, L., et al. (2020). "Functional PVDF/rGO/TiO₂ nanofiber webs for the removal of oil from water." *Polymer* **186**: 122028.
- [32] Jiang, P., et al. (2020). "Research on hydrophobicity of electrospun Fe₃O₄/PVDF nanofiber membranes under different preparation conditions." *Fullerenes, Nanotubes and Carbon Nanostructures* **28**(5): 381-386.
- [33] Tiwari, S., et al. (2019). "Enhanced piezoelectric response in nanoclay induced electrospun PVDF nanofibers for energy harvesting." *Energy* **171**: 485-492.
- [34] Parangusan, H., et al. (2019). "Toward high power generating piezoelectric nanofibers: influence of particle size and surface electrostatic interaction of Ce-Fe₂O₃ and Ce-Co₃O₄ on PVDF." *Acs Omega* **4**(4): 6312-6323.
- [35] Chen, C., et al. (2020). "Enhanced piezoelectric performance of BiCl₃/PVDF nanofibers-based nanogenerators." *Composites Science and Technology* **192**: 108100.
- [36] Sun, B., et al. (2019). "Electrospun poly (vinylidene fluoride)-zinc oxide hierarchical composite fiber membrane as piezoelectric acoustoelectric nanogenerator." *Journal of Materials Science* **54**(3): 2754-2762.

- [37] Mansouri, S., et al. (2019). "Investigation on the electrospun PVDF/NP-ZnO nanofibers for application in environmental energy harvesting." *Journal of Materials Research and Technology* **8**(2): 1608-1615.
- [38] Shuai, C., et al. (2020). "A strawberry-like Ag-decorated barium titanate enhances piezoelectric and antibacterial activities of polymer scaffold." *Nano Energy* **74**: 104825.
- [39] Dandekar, M., et al. (2019). Synthesis and photoluminescence study of electrospun nanofibers of Eu (TTA) 3Phen/PMMA-PVDF composite for photoluminescent fabric designing. AIP Conference Proceedings, AIP Publishing LLC.
- [40] Hanifah, M. F. R., et al. (2019). "Electro-spun of novel PVDF-Pt-Pd/RGO-CeO₂ composite nanofibers as the high potential of robust anode catalyst in direct methanol fuel cell: Fabrication and characterization." *Inorganic Chemistry Communications* **107**: 107487.
- [41] He, W., et al. (2020). "Energetic metastable n-Al@ PVDF/EMOF composite nanofibers with improved combustion performances." *Chemical Engineering Journal* **383**: 123146.
- [42] Shen, X.-l., et al. (2020). "A leaf-vein-like MnO₂@ PVDF nanofiber gel polymer electrolyte matrix for Li-ion capacitor with excellent thermal stability and improved cyclability." *Chemical Engineering Journal* **387**: 124058.
- [43] Li, Y., et al. (2019). "Li₇La₃Zr₂O₁₂ ceramic nanofiber-incorporated composite polymer electrolytes for lithium metal batteries." *Journal of Materials Chemistry A* **7**(7): 3391-3398.
- [44] Li, Z., et al. (2019). "Hierarchical MnO_x@ PVDF/MWCNTs tree-like nanofiber membrane with high catalytic oxidation activity." *Journal of Alloys and Compounds* **780**: 805-815.
- [45] Yang, W., et al. (2020). "GO/Bi₂S₃ Doped PVDF/TPU Nanofiber Membrane with Enhanced Photothermal Performance." *International journal of molecular sciences* **21**(12): 4224.
- [46] Wu, C. M. and M. H. Chou (2016). "Polymorphism, piezoelectricity and sound absorption of electrospun PVDF membranes with and without carbon nanotubes." *Composites Science and Technology* **127**: 127-133.
- [47] Li, Z., et al. (2016). "Fabrication of a polyvinylidene fluoride tree-like nanofiber web for ultra high performance air filtration." *Rsc Advances* **6**(94): 91243-91249.
- [48] Stadlober, B., et al. (2019). "Route towards sustainable smart sensors: ferroelectric polyvinylidene fluoride-based materials and their integration in flexible electronics." *Chemical Society Reviews* **48**(6): 1787-1825.
- [49] Chandrasekaran, S., et al. (2019). "Micro-scale to nano-scale generators for energy harvesting: Self powered piezoelectric, triboelectric and hybrid devices." *Physics Reports* **792**: 1-33.
- [50] Pascariu, P. and M. Homocianu (2019). "ZnO-based ceramic nanofibers: Preparation, properties and applications." *Ceramics International* **45**(9): 11158-11173.

- [51] Ding, H., et al. (2019). "Recent advances in nanomaterial-enabled acoustic devices for audible sound generation and detection." *Nanoscale* **11**(13): 5839-5860.
- [52] Kang, S., et al. (2018). "Transparent and conductive nanomembranes with orthogonal silver nanowire arrays for skin-attachable loudspeakers and microphones." *Science Advances* **4**(8): eaas8772.
- [53] Otani, Y., et al. (2017). "Spin conversion on the nanoscale." *Nature Physics* **13**(9): 829-832.
- [54] Xu, Mingran (2018). Study on the Spin Conversion Induced by Surface Acoustic Waves, The University of Tokyo.
- [55] Tao, L.-Q., et al. (2017). "An intelligent artificial throat with sound-sensing ability based on laser induced graphene." *Nature communications* **8**(1): 1-8.
- [56] Park, S., et al. (2018). "PVDF-based piezoelectric microphone for sound detection inside the cochlea: toward totally implantable cochlear implants." *Trends in hearing* **22**: 2331216518774450.
- [57] Proulx, T. L. and R. Kassayan (2012). Implantable piezoelectric polymer film microphone, Google Patents.
- [58] Ghaffari Bohloli, J., Magnetic Analyst and Isolator Audio Acoustic Spectrum for hearing impaired, H04R00/25, IR, 2019.
- [59] Qiu, X., et al. (2019). "Fully Printed Piezoelectric Polymer Loudspeakers with Enhanced Acoustic Performance." *Advanced Engineering Materials* **21**(11): 1900537.
- [60] Sugimoto, T., et al. (2009). "PVDF-driven flexible and transparent loudspeaker." *Applied Acoustics* **70**(8): 1021-1028.
- [61] Cha, S. N., et al. (2010). "Sound-driven piezoelectric nanowire-based nanogenerators." *Advanced materials* **22**(42): 4726-4730.
- [62] Bae, S.-H., et al. (2013). "Graphene-P (VDF-TrFE) multilayer film for flexible applications." *ACS nano* **7**(4): 3130-3138.
- [63] Wei, Y., et al. (2019). "A wearable skinlike ultra-sensitive artificial graphene throat." *ACS nano* **13**(8): 8639-8647.
- [64] Park, J., et al. (2015). "Fingertip skin-inspired microstructured ferroelectric skins discriminate static/dynamic pressure and temperature stimuli." *Science advances* **1**(9): e1500661.
- [65] Dong, K., et al. (2020). "Fiber/fabric-based piezoelectric and triboelectric nanogenerators for flexible/stretchable and wearable electronics and artificial intelligence." *Advanced materials* **32**(5): 1902549.

- [66] Wu, H., et al. (2016). "Energy harvesters for wearable and stretchable electronics: from flexibility to stretchability." *Advanced materials* **28**(45): 9881-9919.
- [67] Lu, J., et al. (2020). "Electric field-modulated surface enhanced Raman spectroscopy by PVDF/Ag hybrid." *Scientific reports* **10**(1): 1-8.
- [68] Zabek, D., et al. (2017). "Graphene ink laminate structures on poly (vinylidene difluoride)(PVDF) for pyroelectric thermal energy harvesting and waste heat recovery." *ACS applied materials & interfaces* **9**(10): 9161-9167.
- [69] Babaahmadi, V., et al. (2017). "Low temperature welding of graphene on PET with silver nanoparticles producing higher durable electro-conductive fabric." *Carbon* **118**: 443-451.
- [70] Babaahmadi, V., et al. (2018). "Surface modification of PET fabric through in-situ reduction and cross-linking of graphene oxide: Towards developing durable conductive fabric coatings." *Colloids and Surfaces A: Physicochemical and Engineering Aspects* **545**: 16-25.
- [71] Khorsand, S., et al. (2016). "Comparison of Super-Hydrophobicity and Corrosion Resistance of Micro-Nano Structured Nickel and Nickel-Cobalt Alloy Coatings on Copper Substrate." *Journal of Advanced Materials in Engineering (Esteghlal)* **34**(4): 87-105.
- [72] Dumée, L. F., et al. (2015). "Growth of nano-textured graphene coatings across highly porous stainless steel supports towards corrosion resistant coatings." *Carbon* **87**: 395-408.
- [73] Ghafari, E. and N. Lu (2019). "Self-polarized electrospun polyvinylidene fluoride (PVDF) nanofiber for sensing applications." *Composites Part B: Engineering* **160**: 1-9.
- [74] Moazzenchi, B. and M. Montazer (2020). "Click electroless plating and sonopating of polyester with copper nanoparticles producing conductive fabric." *Fibers and Polymers* **21**(3): 522-531.
- [75] Asai, H., et al. (2017). "Effect of melt and solution electrospinning on the formation and structure of poly (vinylidene fluoride) fibres." *RSC advances* **7**(29): 17593-17598.
- [76] Nayak, R., et al. (2012). "Melt-electrospinning of polypropylene with conductive additives." *Journal of Materials Science* **47**(17): 6387-6396.
- [77] Matsouka, D., et al. (2018). "Piezoelectric textile fibres for wearable energy harvesting systems." *Materials Research Express* **5**(6): 065508.
- [78] Samadi, A., et al. (2020). "Piezoelectric performance of microcellular polypropylene foams fabricated using foam injection molding as a potential scaffold for bone tissue engineering." *Journal of Macromolecular Science, Part B* **59**(6): 376-389.
- [79] Bernard, F., et al. (2017). Direct piezoelectric coefficient measurements of PVDF and PLLA under controlled strain and stress. *Multidisciplinary Digital Publishing Institute Proceedings*.

- [80] Gu, L., et al. (2020). "Enhancing the current density of a piezoelectric nanogenerator using a three-dimensional intercalation electrode." *Nature communications* **11**(1): 1-9.
- [81] Jiang, Y., et al. (2018). "Aligned P (VDF-TrFE) nanofibers for enhanced piezoelectric directional strain sensing." *Polymers* **10**(4): 364.
- [82] Chen, X., et al. (2011). "PZT nanoactive fiber composites for acoustic emission detection." *Advanced materials* **23**(34): 3965-3969.
- [83] Chen, X., et al. (2013). "Flexible piezoelectric nanofiber composite membranes as high performance acoustic emission sensors." *Sensors and Actuators A: Physical* **199**: 372-378.
- [84] Wu, S., et al. (2019). "Ceramic nanoparticle-decorated melt-electrospun PVDF nanofiber membrane with enhanced performance as a Lithium-Ion Battery Separator." *Acs Omega* **4**(15): 16309-16317.
- [85] Fang, J., et al. (2013). "Enhanced mechanical energy harvesting using needleless electrospun poly (vinylidene fluoride) nanofibre webs." *Energy & Environmental Science* **6**(7): 2196-2202.
- [86] Xue, J., et al. (2019). "Electrospinning and electrospun nanofibers: Methods, materials, and applications." *Chemical reviews* **119**(8): 5298-5415.
- [87] Katsogiannis, K. A. G., et al. (2016). "Assessing the increase in specific surface area for electrospun fibrous network due to pore induction." *ACS applied materials & interfaces* **8**(42): 29148-29154.
- [88] Tran, C. and V. Kalra (2013). "Fabrication of porous carbon nanofibers with adjustable pore sizes as electrodes for supercapacitors." *Journal of Power Sources* **235**: 289-296.
- [89] Casper, C. L., et al. (2004). "Controlling surface morphology of electrospun polystyrene fibers: effect of humidity and molecular weight in the electrospinning process." *Macromolecules* **37**(2): 573-578.
- [90] Nayani, K., et al. (2012). "Electrospinning combined with nonsolvent-induced phase separation to fabricate highly porous and hollow submicrometer polymer fibers." *Industrial & Engineering Chemistry Research* **51**(4): 1761-1766.
- [91] Szewczyk, P. K., et al. (2020). "Enhanced piezoelectricity of electrospun polyvinylidene fluoride fibers for energy harvesting." *ACS applied materials & interfaces* **12**(11): 13575-13583.
- [92] Zaarour, B., et al. (2018). "Fabrication of a polyvinylidene fluoride cactus-like nanofiber through one-step electrospinning." *RSC advances* **8**(74): 42353-42360.
- [93] Ju, B.-J., et al. (2018). "Development of a superhydrophobic electrospun poly (vinylidene fluoride) web via plasma etching and water immersion for energy harvesting applications." *RSC advances* **8**(50): 28825-28835.

- [94] Shao, H., et al. (2015). "Effect of electrospinning parameters and polymer concentrations on mechanical-to-electrical energy conversion of randomly-oriented electrospun poly (vinylidene fluoride) nanofiber mats." *RSC advances* **5**(19): 14345-14350.
- [95] Lang, C., et al. (2017). "High-output acoustoelectric power generators from poly (vinylidene fluoride-co-trifluoroethylene) electrospun nano-nonwovens." *Nano Energy* **35**: 146-153.
- [96] Martins, M. S., et al. (2019). "Wideband and wide beam polyvinylidene difluoride (PVDF) acoustic transducer for broadband underwater communications." *Sensors* **19**(18): 3991.
- [97] Liu, Q., et al. (2020). "Wireless single-electrode self-powered piezoelectric sensor for monitoring." *ACS applied materials & interfaces* **12**(7): 8288-8295.
- [98] Cui, N., et al. (2015). "High performance sound driven triboelectric nanogenerator for harvesting noise energy." *Nano Energy* **15**: 321-328.
- [99] Qiu, W., et al. (2020). "Sandwich-like sound-driven triboelectric nanogenerator for energy harvesting and electrochromic based on Cu foam." *Nano Energy* **70**: 104543.
- [100] Shao, H., et al. (2020). "Efficient conversion of sound noise into electric energy using electrospun polyacrylonitrile membranes." *Nano Energy* **75**: 104956.
- [101] Karim, N., et al. (2019). "All inkjet-printed graphene-silver composite ink on textiles for highly conductive wearable electronics applications." *Scientific reports* **9**(1): 1-10.
- [102] Moazzenchi, B. and M. Montazer (2019). "Click electroless plating of nickel nanoparticles on polyester fabric: Electrical conductivity, magnetic and EMI shielding properties." *Colloids and Surfaces A: Physicochemical and Engineering Aspects* **571**: 110-124.
- [103] Ahn, Y.-J., et al. (2012). "Preparation of conductive nanoweb through electrospinning followed by electroless silver-plating and its application as dry-type electrode for ECG measurement." *Textile Science and Engineering* **49**(1): 47-55.
- [104] Harirforush, N., et al. (2018). Investigation of acoustic behavior of piezoelectric nanofibers, Amirkabir University of Technology.